Precambrian Research 364 (2021) 106363

Contents lists available at ScienceDirect

Precambrian Research

journal homepage: www.elsevier.com/locate/precamres

Recognition of the "Great Unconformity" in the eastern Sino-Korean Block: Insights from the Taebaek Group, Korea

Jeong-Hyun Lee [a,b], Min-Kyu Oh [b], Taejin Choi [c,*]

[a] Department of Geological Sciences, Chungnam National University, Daejeon 34134, Republic of Korea
[b] Department of Astronomy, Space Science and Geology, Chungnam National University, Daejeon 34134, Republic of Korea
[c] Department of Advanced Energy Engineering, Chosun University, Gwangju 61542, Republic of Korea

ARTICLE INFO

Keywords:
Taebaek Group
Jangsan Formation
Myeonsan Formation
Myobong Formation

ABSTRACT

Precambrian and Cambrian rocks are often separated by the "Great Unconformity", a global contact that can represent a gap spanning hundreds of millions of years of time. A coeval unconformity in the Sino-Korean Block has recently been documented from several different areas of China; however, the stratigraphic position of this boundary in the eastern margin of the Sino-Korean Block in the Taebaek Group, central-eastern Korea, is still elusive. We present an integrated approach incorporating detailed field observations, sedimentary petrography, and detrital zircon geochronology on the basal stratigraphic units of the Taebaek Group (Jangsan, Myeonsan, and Myobong formations) to resolve this issue. In contrast to the traditional view that all three formations are of early Cambrian age, that the Myeonsan Formation is a lateral equivalent of the Jangsan Formation, and that the Myobong Formation conformably overlies the other two formations, our data indicate that the Myeonsan Formation can be a lateral equivalent of the basal Myobong Formation. We propose that the Great Unconformity possibly lies between the Jangsan and Myeonsan/Myobong formations: the Jangsan Formation is probably of Precambrian age, and the Myeonsan and Myobong formations are early Cambrian in age. This result suggests that the Great Unconformity on the Sino-Korean Block extends to the eastern margin of the block in the Korean Peninsula. The recognition of the Great Unconformity in the Taebaek Group will help to clarify the stratigraphic correlation, tectonic history, and paleogeographic reconstruction of the eastern Sino-Korean Block during the Cambrian.

1. Introduction

The "Great Unconformity" between Precambrian and Cambrian strata has been identified throughout the world, including in Laurentia, Gondwana, Baltica, Avalonia, and Siberia. The unconformity resulted from the break up of Rodinia, formation of the Gondwana as well as global eustatic sea-level rise (Brasier and Lindsay, 2001; Peters and Gaines, 2012; DeLucia et al., 2018). Many recent studies have emphasized the importance of the Great Unconformity in terms of stratigraphy, evolution of organisms, sequence stratigraphy, and paleoceanography, as well as ore geology (Peters and Gaines, 2012; Parnell et al., 2014; Karlstrom et al., 2018; Keller et al., 2019; Barnes et al., 2020; Shahkarami et al., 2020). The Sino-Korean Block, one of the oldest cratons in the world (Zhao et al., 2005), was a microcontinent located near or at the eastern margin of Gondwana during the early Paleozoic (McKenzie et al., 2011; Han et al., 2016; Zhao et al., 2021). Thick Meso- to Neoproterozoic strata were deposited throughout the Sino-Korean Block, which are unconformably overlain by Cambro–Ordovician strata (Meng et al., 1997; Xiao et al., 1997, 2014; Chough et al., 2010; Meng et al., 2011; He et al., 2017; Wan et al., 2019; Zhai et al., 2019; Zuo et al., 2019; Li et al., 2020a; Li et al., 2020b; Zhang et al., 2020). The Precambrian–Cambrian boundary on the Sino-Korean Block commonly occurs as a cryptic disconformity, and recognizing this surface thus requires integrated investigations using a variety of methods (e.g., Xiao et al., 2014; He et al., 2017; Wan et al., 2019). Compared with Laurentia, where the Great Unconformity has been recognized and studied over the last few decades (Shahkarami et al., 2020 and references therein), further research is required to understand the nature of the Great Unconformity on the Sino-Korean Block.

In the eastern margin of the Sino-Korean Block (Korean Peninsula), lower Paleozoic strata are represented by the Taebaek Group (lower Cambrian–Middle Ordovician) (Fig. 1) (Choi et al., 2004; Kwon et al.,

* Corresponding author.
E-mail addresses: jeonghyunlee@cnu.ac.kr (J.-H. Lee), minkyuoh@g.cnu.ac.kr (M.-K. Oh), tchoi@chosun.ac.kr (T. Choi).

https://doi.org/10.1016/j.precamres.2021.106363
Received 9 February 2021; Received in revised form 6 August 2021; Accepted 12 August 2021

2006). The lowermost part of the group comprises the Jangsan and Myeonsan formations, which both unconformably overlie Paleoproterozoic basement rocks of the Yeongnam Massif (J.Y. Kim and Cheong, 1987; Woo et al., 2006). These two formations are laterally bounded by a major right-lateral strike-slip fault (the Dongjeom Fault; Fig. 1) and are traditionally considered to be lateral equivalents (Cheong et al., 1973; Yun, 1978; J.Y. Kim and Cheong, 1987; J.Y. Kim, 1991; Chough et al., 2000; Y.I. Lee and J.I. Lee, 2003; Choi et al., 2004; Kwon et al., 2006; Woo et al., 2006; Chough, 2013). The Myeonsan Formation gradually fines upward into the overlying Myobong Formation, and there is a general consensus that these two formations are conformable and are of early Cambrian age (Choi et al., 2004; Kwon et al., 2006; Y.I. Lee et al., 2016c).

However, the relationship between the Jangsan and Myobong formations has been questioned over the last few decades. Although these two formations have traditionally been considered to be conformable (Kobayashi, 1930; Son and Cheong, 1965; Kobayashi, 1966; Cheong, 1969; Yun, 1978; J.Y. Kim and Cheong, 1987; Choi et al., 2004), Y. Kim and Lee (2006) reported outcrops with an "unconformable" boundary between the Jangsan and Myobong formations and suggested that there was a major time gap between these two formations. Y.I. Lee et al. (2012) reported an abrupt change in detrital zircon age spectra from the two formations and suggested that this change may indicate an unconformable relationship between them. However, Y. Kim and Lee (2006) did not present detailed outcrop observations of the boundary, and their outcrops are only poorly exposed. In fact, one of the outcrops (the west Dongjeom section; Fig. 1B, D) reported by Y. Kim and Lee (2006) later turned out to be a faulted contact (Chough et al., 2016). H.S. Kim et al. (2019) suggested that differences in the sediment grain sizes could reflect provenance changes, and thus the abrupt changes in sediment provenance reported by Y.I. Lee et al. (2012) are not solid evidence that these two formations are unconformable. In this study, we present the evidence that the Jangsan and Myobong formations are unconformable based on detailed outcrop and petrographic observations, as well as detrital zircon analyses. Positioning the Great Unconformity on the eastern Sino-Korean Block will help to constrain the geographic extent of the unconformity and the geochronologic magnitude of the unconformity-forming event across the Precambrian–Cambrian boundary.

2. Geological setting

Eastern Asia (including most of Korea, China, and Japan) consisted of two major blocks during the early Paleozoic: the Sino-Korean (or North China) Block and the South China Block, which collided during the Permian–Triassic (Fig. 1A) (Yin and Nie, 1993; Chough et al., 2000). Both blocks were either microcontinents located near the Gondwana Supercontinent or parts of the supercontinent during the early Paleozoic (McKenzie et al., 2011). The Korean Peninsula consists of three major massifs, which are from north to south the Nangrim, Gyeonggi, and Yeongnam massifs (Chough et al., 2000). There has been controversy on the paleogeographic affinities of these massifs, except for the Nangrim Massif, which is an eastward extension of the Sino-Korean Block (Chough et al., 2000; Zhai et al., 2019). The Gyeonggi massif has been

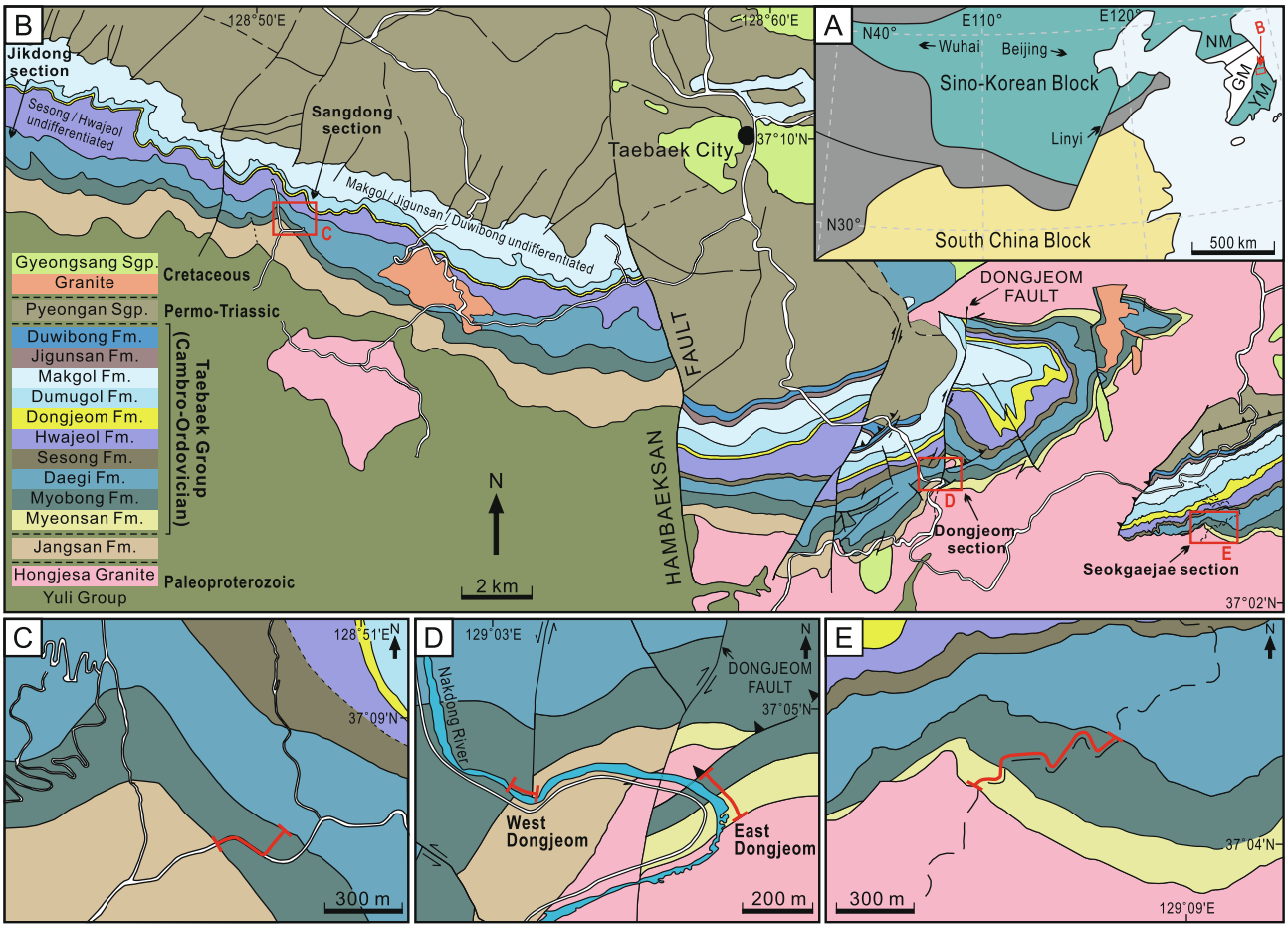

Fig. 1. Geological map of the Taebaeksan Basin. (A) Location of the Taebaeksan Basin in the Sino-Korean block. NM, Nangrim Massif; GM, Gyeonggi Massif; YM, Yeongnam Massif. (B) Geological map of the Taebaeksan Basin. The locations of the Sangdong (37°08′44″N 128°50′35″E), Dongjeom (37°04′53″N 129°03′16″E), and Seokgaejae (37°04′05″N 129°08′31″E) sections are marked with arrows. (C–E) Close-up maps of (C) the Sangdong section, (D) the Dongjeom section, and (E) the Seokgaejae section. Maps modified after GICTR (1962), Choi et al. (2004), and Chough (2013).

correlated with both the Sino-Korean Block and the South China Block by different studies (Choi, 2019 and references therein). This is also the case for the Yeongnam massif, but we consider this massif to be associated with the Sino-Korean block on the basis of sedimentological and paleontological evidence (Chough, 2013).

The Cambro–Ordovician Joseon Supergroup occurs in the Taebaeksan and Pyeongnam basins in the Korean Peninsula, which are parts of the Yeongnam and Nangrim massifs, respectively (Fig. 1). The Taebaek Group comprises mixed siliciclastic–carbonate successions of the Jangsan/Myeonsan, Myobong, Daegi, Sesong, Hwajeol, Dongjeom, Dumugol, Makgol, Jigunsan, and Duwibong formations in stratigraphic ascending order (Choi et al., 2004; Choi and Chough, 2005). In the southeastern Taebaeksan Basin, the Jangsan Formation occurs west of the north–south-trending Dongjeom Fault (J.Y. Kim and Cheong, 1987) and unconformably overlies metamorphosed sedimentary rocks of the Paleoproterozoic (ca. 2010–2180 Ma, Y.I. Lee et al., 2011; 1838 ± 5–1878 ± 5.2 Ma, Jeong, 2020) Yuli Group and the Paleoproterozoic Hongjesa granitic gneiss ($2013^{+30}/_{-24}$ Ma) (H.-S. Lee et al., 2010). The Myeonsan Formation is found east of the Dongjeom Fault (Cheong et al., 1973; J.Y. Kim and Cheong, 1987) and unconformably overlies the Hongjesa granitic gneiss, without the Jangsan Formation. The Dongjeom Fault is thought to be of Cretaceous age (J.H. Kim et al., 2000). Both the Jangsan and Myeonsan formations are stratigraphically overlain by the black "shales" or "slates" of the Myobong Formation. The Jangsan/Myeonsan formations occur parallel to the Myobong Formation in geologic maps, and their strikes and dips are generally similar (Fig. 1) (GICTR, 1962). Based on these observations, the Jangsan and Myeonsan formations are traditionally considered as lateral equivalents (J.Y. Kim, 1991; Choi et al., 2004; Choi and Chough, 2005; Kwon et al., 2006; Woo et al., 2006).

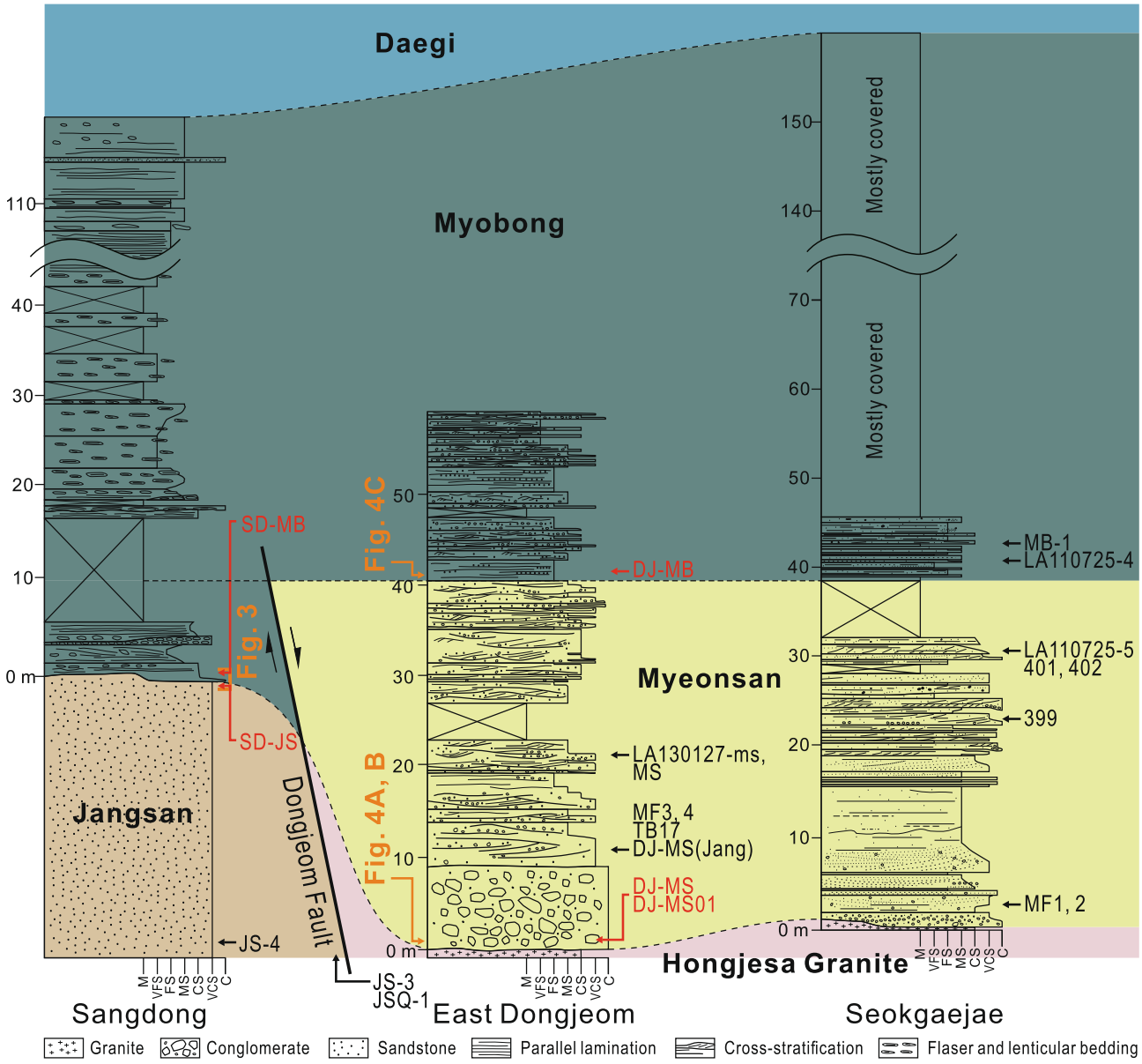

Fig. 2. Sedimentological logs of the Sangdong (modified after Oh, 2020), east Dongjeom (modified after Woo et al., 2006), and Seokgaejae (modified after Choi et al., 2004) sections. Sampled horizons for the detrital zircon analyses of this study (red arrows; SD-JS, SD-MB, DJ-MS, DJ-MS01, DJ-MB) and previous studies (JS-3, JS-4, MB-1: Y.I. Lee et al., 2012; MF1, 2, 3, 4: H.S. Kim et al., 2013; LA110725-4, 5, LA130127-ms, Y.I. Lee et al., 2016c; JSQ-1: S.W. Kim et al., 2017; DJ-MS (Jang): Jang et al., 2018; 399, 401, 402, TB17: Cho et al., 2021) are marked. JS-3 and JSQ-1 are from the Jangsan Formation of the west Dongjeom section. M: mudstone, VFS: very fine sandstone, FS: fine sandstone, MS: medium sandstone, CS: coarse sandstone, VCS: very coarse sandstone, C: conglomerate. (For interpretation of the references to colour in this figure legend, the reader is referred to the web version of this article.)

A platform-wide transgression began in the early Cambrian (Stage 3 or 4) and covered a vast area of the Sino-Korean Block (Meng et al., 1997). The Jangsan and Myeonsan formations are previously regarded to represent initial stage of this transgression event (Kwon et al., 2006; Woo et al., 2006). The Jangsan Formation comprises milky white to pinkish coarse-grained quartzose sandstone with minor well-rounded quartzite and gneiss pebbles (Yun, 1978; Woo et al., 2006). Sedimentary structures such as trough and tabular cross-stratification are commonly found in the formation, and are interpreted to have formed in inner-shelf to nearshore environments (Woo et al., 2006). The Myeonsan Formation consists of basal conglomerate, dark gray sandstone, and mudstone formed in a restricted embayment with tidal influence (J.Y. Kim, 1991; Woo et al., 2006). The Myobong Formation comprises various lithofacies ranging from mudstone to dark gray gravelly sandstone deposited in peritidal to shoal environments (Fig. 2) (Oh, 2020), and is early–middle Cambrian in age (Cambrian Stage 3?–Wuliuan) based on the occurrences of the *Redlichia*, *Elrathia*, *Mapania* (?), and *Bailiella* trilobite biozones (Kobayashi, 1966; Choi et al., 2016).

Classically, the Taebaek Group was described from the Dongjeom, Sangdong, and Jikdong areas, of which the Dongjeom and Sangdong sections contain the basal succession of the group (Choi et al., 2004) (Fig. 1). Stratotype sections for the Taebaek Group were proposed in the Dongjeom and Sangdong areas (Kobayashi, 1930, 1966), but the original outcrops have been partly destroyed due to weathering and construction. As a result, outcrops are at the present day only sporadically exposed, with numerous stratigraphic gaps. Instead, the Seokgaejae section has been proposed as a principal reference section for the entire Taebaek Group (Choi et al., 2004). We describe these three main sections, the Sangdong, Dongjeom, and Seokgaejae sections, focusing on the basal units (the Jangsan, Myeonsan, and Myobong formations).

The Sangdong section is located in the westernmost part of the study area (Fig. 1B, C). This section has been described as containing the Jangsan and Myobong formations, without the Myeonsan Formation (Kwon et al., 2006). In this section, the Jangsan Formation is about 200 m thick and is stratigraphically overlain by the Myobong Formation. The Myobong Formation is about 120 m thick in the Sangdong section (Fig. 2) (Oh, 2020).

The Dongjeom section is located approximately 8 km south of Taebaek city, and occurs along the Nakdong River (Fig. 1B, D). The lowermost part of the Taebaek Group is identified from two subsections of the Dongjeom section, located west and east of the Dongjeom Fault, respectively. In the west Dongjeom section, an east–west-trending fault contact between the Jangsan Formation and the upper Myobong Formation occurs along the stream (Chough et al., 2016). In this section, the Jangsan Formation is structurally thickened by repeated thrust faults (J.-H. Lee et al., 2016a). In the east Dongjeom section, the Myeonsan Formation (ca. 40 m thick) unconformably overlies the Hongjesa granitic gneiss with ~4 m thick basal conglomerate (J.-Y. Kim and Cheong, 1987; Woo et al., 2006), and grades into the overlying finer-grained Myobong Formation (ca. 20 m thick) (Fig. 2). The Dongjeom Fault separates the west and east subsections, marking the lower boundary of the Jangsan Formation to the west and the upper boundary of the Myobong Formation to the east.

The Seokgaejae section is located in the easternmost part of the study area (Fig. 1B, E), and contains 38.6-m-thick coarse sandstone of the Myeonsan Formation unconformably overlying the Hongjesa granitic gneiss with a ~1 m thick basal conglomerate (Fig. 2) (Choi et al., 2004, their fig. 3). The overlying Myobong Formation is mostly covered in the Seokgaejae section, and is assumed to be about 130 m thick (Choi et al., 2004). The base of the Myobong Formation is placed at the first occurrence of dark gray, homogeneous mudstone (Choi et al., 2004).

3. Methods

The contact between the Jangsan and Myobong formations is found in the Sangdong section, which runs along a stream (Fig. 1). The outcrop has been studied in order to reveal the nature of this boundary, and sketches and sedimentological logs were drawn on the basis of detailed observations (Figs. 2, 3). Two samples containing the exact boundary between the Jangsan and Myobong formations were collected from the outcrop and prepared as slabs (Fig. 5). Thin sections corresponding to the polished slab surfaces were made to observe microscale structures.

Samples for detrital zircon analysis were collected from the Jangsan, Myeonsan, and Myobong formations in the Sangdong and Dongjeom areas. In the Sangdong section, sandstone samples from the Jangsan (SD-JS) and Myobong formations (SD-MB) were collected ~0.5 m below and above the formation boundary, respectively (Figs. 2, 3A). In the east Dongjeom section, two boulder-sized sandstone clasts from the basal Myeonsan Formation (DJ-MS and DJ-MS01) and from sandstone in the Myobong Formation in the upper part of the outcrop (DJ-MB) were collected (Fig. 2). Thin sections were prepared from the same samples for petrographic observation and identification of modal composition using the traditional point-counting method.

Detrital zircon grains were separated from the collected samples using the conventional heavy-mineral separation method at the Geological Department at Lund University, Sweden. The zircon was handpicked from the concentrates, mounted in epoxy, and polished. Transmitted light microscopy, secondary emission (SE), cathodoluminescence (CL), and back-scattered electron (BSE) imaging were applied to reveal the internal structures of the zircon and to select analytical spot positions. SE, CL, and BSE imaging were performed using the High-Resolution field-emission–scanning electron microscope (FE–SEM; Tescan Mira 3, Brno, Czech Republic) at Lund University.

U–Pb isotope analyses were carried out in the Laser Ablation Inductively Coupled Plasma Mass Spectrometry (LA–ICP–MS) laboratory at Lund University. The laboratory includes a Teledyne Photon Machines G2 (Teledyne Technologies, Omaha, USA) laser coupled to a Bruker Aurora Elite quadrupole ICP–MS (Bruker Daltonics, Bremen, Germany). Instrument tuning was aimed at obtaining high and stable signal counts on lead isotopes, on low oxide production (below 0.5% monitoring $^{238}U/^{238}U^{16}O$ and $^{232}Th/^{232}Th^{16}O$), and on Th/U ratios of 1 using NIST612 for the standard. The primary and secondary reference standards for the analytical session were the GJ-1 (Jackson et al., 2004) and 91,500 (Wiedenbeck et al., 1995) natural zircon, respectively. The analytical results of the reference samples are shown in Supplementary Table 2. Each analysis was done with 300 shots at 10 Hz with a fluence between 2.5 J/cm^2, measuring baseline compositions for 30 s before each measurement, and subtraction was performed with a step-forward approach. Common Pb was monitored by measuring ^{202}Hg and mass 204 ($^{204}Hg + {}^{204}Pb$). Data reduction was made with Iolite using the X_U_Pb_Gerchron4 DSR (Paton et al., 2010; Paton et al., 2011), and the common-Pb correction was done using the VizualAge DRS by Petrus and Kamber (2012). Decay constant values (λ) of ^{238}U and ^{235}U used to calculate the zircon ages are $1.55125 * 10^{-10}$/yr and $9.8485 * 10^{-10}$/yr, respectively (Steiger and Jäger, 1977). All uncertainties of the isotopic ratios and ages are 2σ levels. For the zircon ages older and younger than 1000 Ma, $^{207}Pb/^{206}Pb$ and $^{206}Pb/^{238}U$ ages are used respectively. Discordance (%) of the zircon ages were calculated as [1−($^{206}Pb/^{238}U$ age)/($^{207}Pb/^{235}U$ age)] * 100 and [1−($^{206}Pb/^{238}U$ age)/($^{207}Pb/^{206}Pb$ age)] * 100 with ages younger and older than 1000 Ma, respectively. The kernel density estimates (Vermeesch, 2013) were constructed using the $^{206}Pb/^{238}U$ ages and $^{207}Pb/^{206}Pb$ ages for zircon with the same criteria.

4. Field and petrographic observations

4.1. Field observations

The studied outcrop in the Sangdong section that contains the Jangsan–Myobong boundary comprises an approximately 2-m-thick continuous succession of the light gray to reddish quartzose coarse sandstone (uppermost Jangsan Formation) overlain by the dark gray

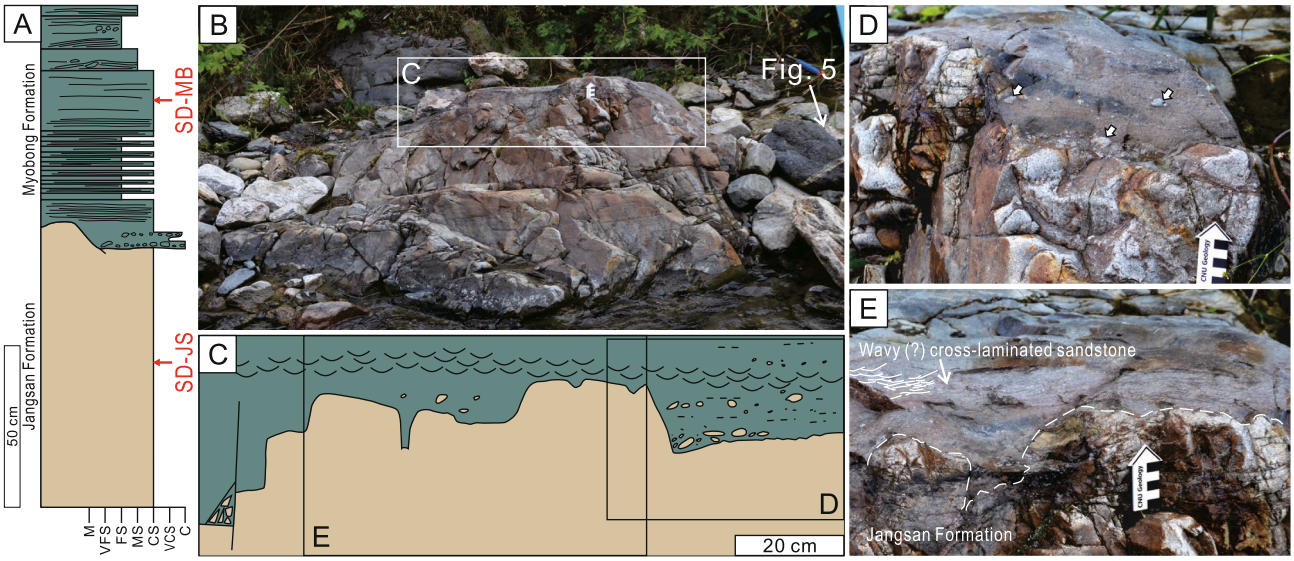

Fig. 3. Details of the Sangdong section that contains the Jangsan–Myobong boundary. (A) Sedimentary log, (B) photograph of the boundary interval shown in (A), and (C) an interpretative sketch of part of the interval. M: mudstone, VFS: very fine sandstone, FS: fine sandstone, MS: medium sandstone, CS: coarse sandstone, VCS: very coarse sandstone, C: conglomerate. (D, E) Details of the outcrop, showing the irregular boundary between the Jangsan and Myobong formations. Note the occurrence of sandstone pebbles (arrows) in the basal Myobong Formation that might have been derived from the underlying Jangsan Formation in (D). (E) Wavy (?) cross-laminated sandstone (partly linedrawn) occurring in the upper part of the topographic low. Scales in centimeters.

gravelly to medium sandstone with rare pebbles (lowermost Myobong Formation) (Fig. 3). The Myobong Formation gradually fines upward, but never contains grains smaller than fine sand within the study interval (Fig. 3A). This boundary shows centimeter- to decimeter-scale irregular topography with a sharp boundary (Fig. 3B, C). Clast-bearing gravelly sandstone with crude lamination has filled in the topographic low (Fig. 3D). The clasts are gravel to pebble size and are generally aligned parallel to subparallel to the bedding plane, and composed of coarse sandstone that is similar to the Jangsan Formation below. In the upper part of the topographic low, slightly wavy (?) cross-laminated sandstone either directly overlies the Jangsan Formation or laterally extends and covers the depression-filling gravelly sandstone (Fig. 3E). This "wavy" cross-lamination could have been affected by pressure solution, as inferred from its sutured fabric that resembles stylolites. Still, its lateral persistence suggests that the "wavy" sandstone is stratigraphically in situ (Fig. 3C).

In the east Dongjeom section, the basal conglomerate of the Myeonsan Formation unconformably overlies the Precambrian Hongjesa granite (Fig. 4A). The conglomerate consists of various sub- to well-rounded cobble- to boulder-sized clasts including sandstone, quartzite, chert, and granitic gneiss. Notably, some boulder-sized sandstone clasts are dominated by coarse- to very coarse sand-sized quartz with apparent stratification (Fig. 4B). The upper part of the Myeonsan Formation in the Dongjeom section consists of fine- to medium-sand-sized sandstone alternating with siltstone layers, and the boundary between the Myeonsan and overlying Myobong formations is placed at the first occurrence of a thick dark gray silt- to fine sandstone bed (Fig. 4C). Overall, the general sedimentary succession of the Myeonsan and Myobong formations in the Dongjeom section is similar to that of the Seokgaejae section (Fig. 2) (Kwon et al., 2006).

4.2. Petrographic observation

4.2.1. Slab and thin-section analysis of the Jangsan–Myobong boundary

The slab analysis of the boundary sample acquired from the Sangdong section shows that there is a clear boundary between the underlying brownish to grayish sandstone of the Jangsan Formation and the dark gray sandy conglomerate of the Myobong Formation (Fig. 5A). The layer above (Myobong Formation) comprises a matrix of coarse silt to very fine sand-sized detrital ilmenite and some quartz and feldspar with moderately rounded to sub-angular quartzose sandstone and quartzite clasts (Fig. 5B, C). The Jangsan sandstone and the sandstone clasts in the Myobong Formation are petrographically similar, with quartz overgrowth observed from both of them. Deformation-induced features (e.g., cataclastic foliation, fault gauge) are not observed in thin section along the boundary (Fig. 5C), suggesting the boundary is not produced from a post-depositional tectonic event (cf. Chough et al., 2016).

4.2.2. Microscale observation

The sample from the Jangsan Formation (SD-JS) dominantly consists of monocrystalline (80%; 465/581) and polycrystalline (11.2%; 65/581) quartz with a substantial amount of matrix (8.8%; 51/581 points) (Fig. 6). This makes the rock a quartz wacke. Grains range from fine to very coarse sand, but the dominant component is moderately to well sorted, subangular to moderately rounded coarse sand (Fig. 7A). Some quartz grains show syntaxial overgrowth. Previous studies suggested that the matrix (mainly sericite) constitutes as much as 30% of the volume, which could have resulted from diagenesis of feldspar and lithic fragments (Y.I. Lee et al., 2016b). Remnants of original feldspar grain shapes can also be locally observed in our samples (Fig. 7A). If all of the matrices had originally been feldspar, then the Jangsan sandstone can be classified as quartz arenite to subarkose. No evidence of organisms (e.g., bioclasts, bioturbation) was found in the Jangsan sandstone. Overall, the petrographic characteristics of our Jangsan sample are very similar to those of the Jangsan Formation at other localities (Y.I. Lee et al., 2012) (Fig. 6).

The sample from the basal Myobong Formation in the Sangdong section (SD-MB) is poorly sorted, medium to very coarse sandy siltstone mainly consisting of a silt-sized matrix (73.1%; 471/644) with quartz (17.9%; 115/644) and detrital ilmenite (9%; 58/644) grains, in addition to a substantial amount of secondary skarn minerals (Fig. 7B). Under the SEM, these ilmenite grains are generally moderately to well-rounded and very fine sand-sized, and do not show interlocking texture, suggesting that these are detrital sediments (cf. H.S. Kim et al., 2013). Gravel-size clasts consisting of quartzose sandstone with abundant matrix are common (Fig. 7B), and are similar in composition to the cobble- to boulder-sized sandstone clasts of the basal Myeonsan Formation (Y. Kim and Y.I. Lee, 2006). The sample from the Myobong Formation in the

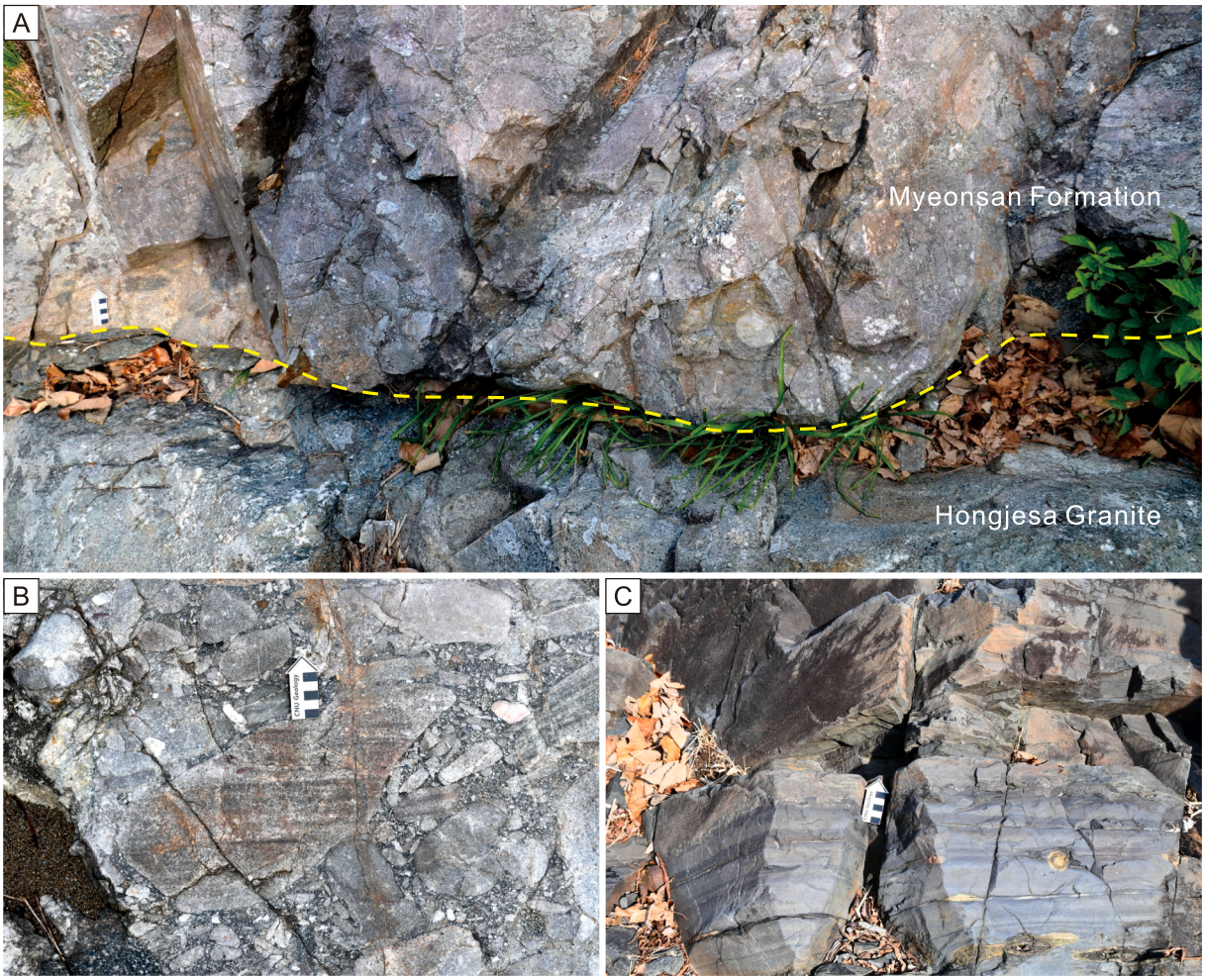

Fig. 4. Outcrop photographs of the east Dongjeom section. (A) Unconformity between the Paleoproterozoic Hongjesa Granite and basal conglomerate of the Myeonsan Formation. Samples DJ-MS and DJ-MS01 are collected from this outcrop. (B) Boulder-sized sandstone clasts in the basal conglomerate. Note the occurrence of distinctive lamination within the sandstone clast. (C) Photograph of the lower Myobong Formation, consisting of dark-colored fine sandstone below and coarse sandstone above, from which sample DJ-MB was collected. Scales in centimeters.

Dongjeom section (DJ-MB) is fine to medium sandy siltstone consisting of monocrystalline (29.7%; 179/602) and polycrystalline (6.5%; 39/602) quartz, detrital ilmenite (28.2%; 170/602), minor feldspar (0.03%; 2/602), and rock fragments (1.8%; 11/602) with abundant matrix (33.4%; 201/602) (Fig. 7D).

The petrography of Myeonsan sandstone reported by J.Y. Kim (1991) and H.S. Kim et al. (2013) indicates that the sandstone is immature litharenite. The main components of the sandstone are subangular to subrounded quartz (18%–53%), feldspar (~13%), rock fragments (~13%), and matrix (mainly micas and clay minerals; 3%–26%), with abundant (locally up to 60%) opaque minerals (ilmenite and hematite) (J.Y. Kim, 1991; H.S. Kim et al., 2013). Similar to our Myobong samples, ilmenite grains are moderately to well rounded, suggesting a detrital origin. Although the Myobong sandstone from the Seokgaejae section was previously identified as feldspathic arenite by Y.I. Lee et al. (2016c), they counted matrix ("near completely sericitized" in their word) as feldspar (Fig. 6). If these "feldspar" are not counted, the Myobong sandstone from the Seokgaejae section is similar in composition to our Myobong sandstone from the Dongjeom section. In contrast, the sampled Myeonsan sandstone clasts as part of this study are petrographically indistinguishable from the Jangsan Formation (Fig. 7C). The DJ-MS and DJ-MS01 clasts contain monocrystalline quartz (DJ-MS: 64.5%, 409/634, DJ-MS01: 62.9%, 371/590), polycrystalline quartz (DJ-MS: 19.6%, 124/634; DJ-MS01: 25.1%, 148/590), and matrix (DJ-MS: 15.9%, 101/634; DJ-MS01: 12%, 71/590). Quartz grains in both samples are commonly moderately rounded to sub-angular and medium to very coarse sand-sized.

5. Detrital zircon U–Pb geochronology

We obtained a total of 787 U–Pb ages from five samples (Supplementary Table 1 and Supplementary Fig. 1). Among the analytical results, 337 concordant to slightly discordant (<10% discordance) ages were selected, ranging from Archean to Cambrian in age. The zircon grains are largely subangular to rounded (Fig. 8), although the Paleozoic zircon grains have more angular and euhedral morphologies than the Precambrian grains. Many of the Paleoproterozoic to Archean zircon grains are subangular or rounded, and some of the rounded zircon are fragmentary, which suggests possible recycling. Most of the zircon have oscillatory growth or patchy zoning, which are indicative of a magmatic origin (Corfu et al., 2003).

5.1. Jangsan Formation

Of the 160 analyses of detrital zircon from sample SD-JS from the Jangsan Formation (Fig. 8), 70 grains show concordant U–Pb ages ranging from 2793 to 1849 Ma (Fig. 9; Supplementary Table 1). Two Phanerozoic zircon ages of 326 ± 14 Ma and 240 ± 7 Ma obtained from this sample are not dealt with in this study because they are much younger than the depositional age of the overlying Cambrian Myobong

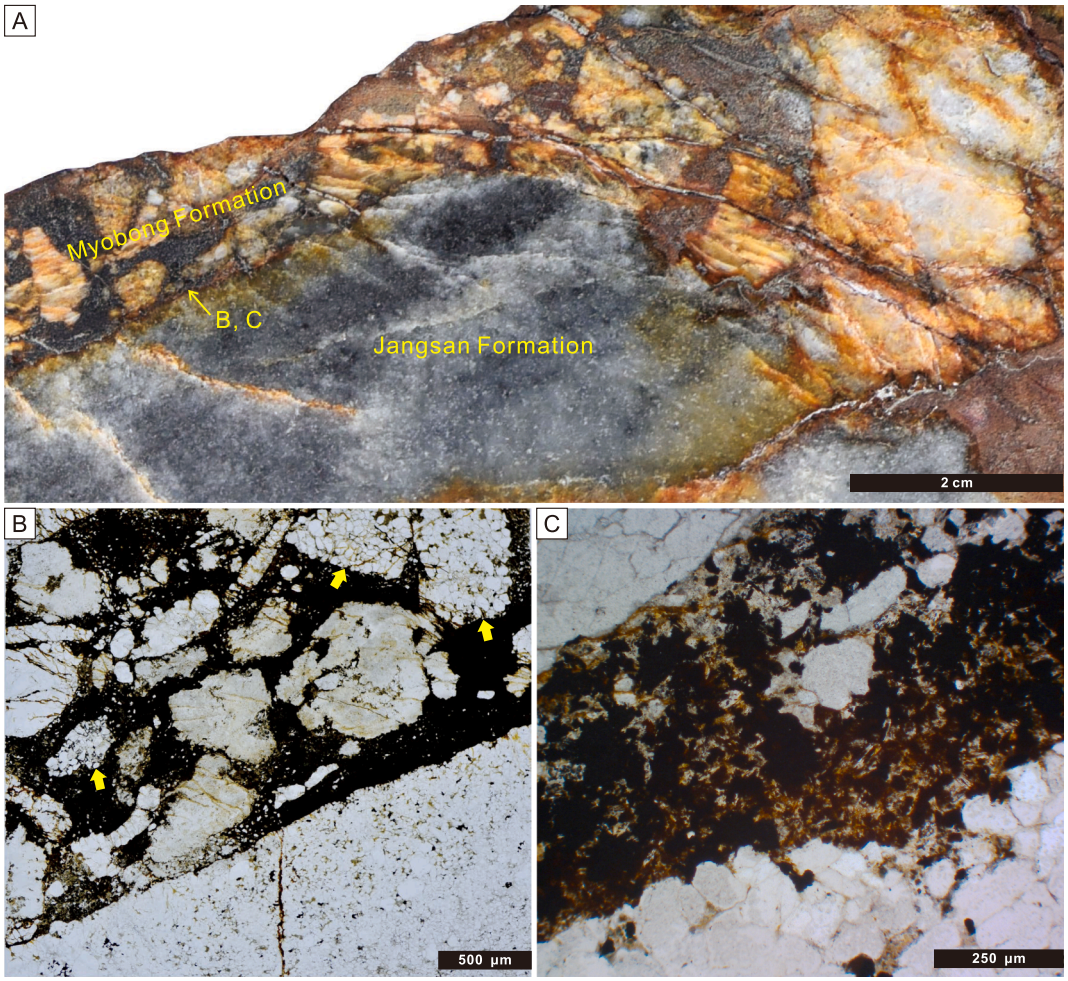

Fig. 5. Slab photograph and thin-section photomicrographs of the Jangsan–Myobong boundary from the Sangdong section. (A) Scan of the slab showing the boundary between quartzose sandstone of the Jangsan Formation below and dark gray conglomerates of the Myobong Formation above. (B) Photomicrograph of the sharp lithologic boundary. Sandstone clasts that are similar to the Jangsan Formation (arrows) are commonly found in the Myobong Formation. (C) Close-up of the boundary. The dark matrix consists of various opaque minerals, including detrital ilmenite.

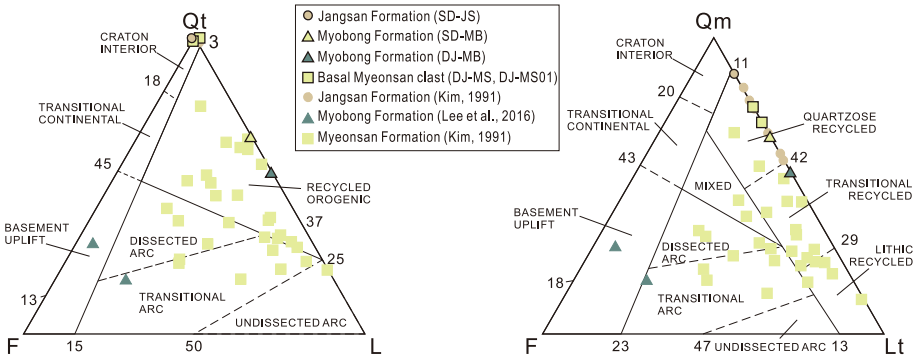

Fig. 6. Total quartz–feldspar–non-quartzose lithic grains (Qt–F–L) and monocrystalline quartz–feldspar–total lithic grains (Qm–F–Lt) diagrams of the Jangsan, Myeonsan, and Myobong sandstone. Previously published data for the Jangsan, Myeonsan (J.Y. Kim, 1991), and Myobong (Y.I. Lee et al., 2016c) formations are also presented. Note that the Myobong samples of Y.I. Lee et al. (2016c, p. 774) counted matrix as feldspar, making them feldspartic arenite.

Formation. Those ages might have been affected by later events after the burial of the Jangsan Formation. Two dominant age groups were found: Paleoproterozoic (67%) and Archean (33%). The zircon age spectrum shows the most prominent peak at 2495 Ma with a relatively short but broad peak at 1920 Ma. This zircon age population is generally similar to that from the same location of the Jangsan Formation reported by Y.I. Lee et al. (2012), as well as to those from other localities of the Jangsan Formation (S.W. Kim et al., 2017; H.S. Kim et al., 2019; Cho et al., 2021; C. Lee et al., in press), which exhibited bimodal zircon age peaks at ca. 1900 and 2500 Ma.

5.2. *Myobong Formation*

From the Myobong Formation, 320 U–Pb analyses on the detrital

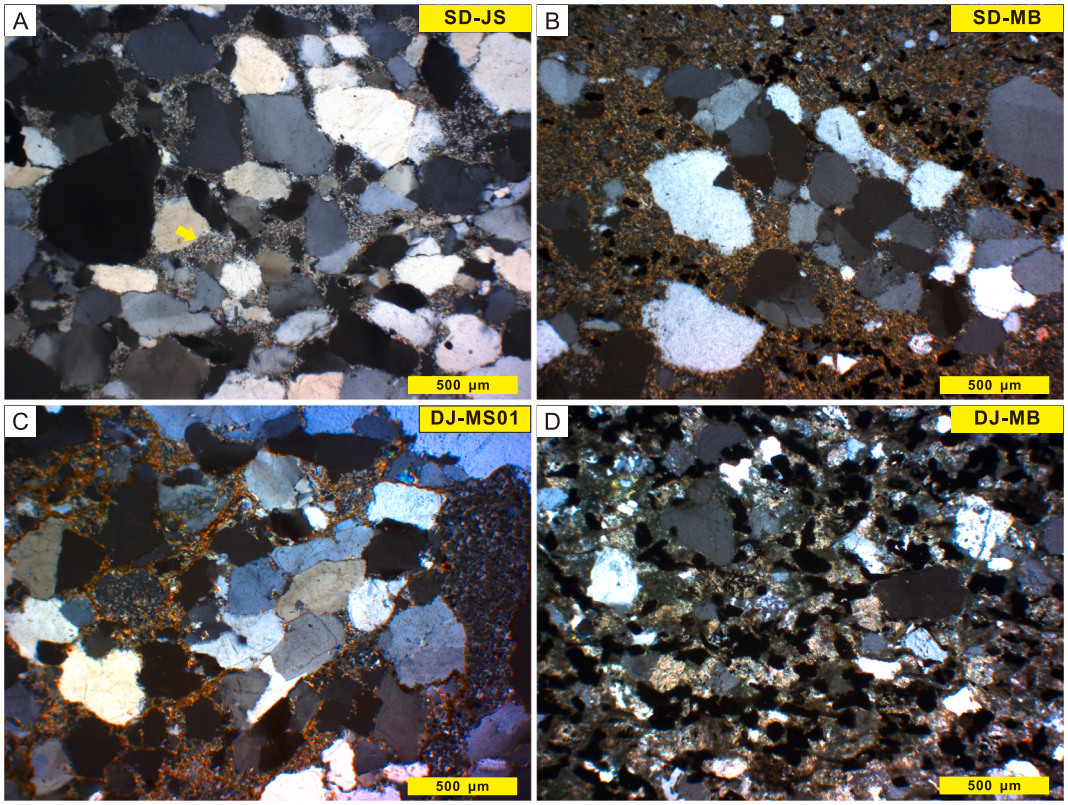

Fig. 7. Photomicrographs taken with cross-polarized light. (A) Jangsan Formation (SD-JS) with possible feldspar pseudomorph (arrow). (B) Myobong Formation from the Sangdong section (SD-MB) with a large sandstone clast resembling the Jangsan Formation. (C) Sandstone clast of the Myeonsan Formation (DJ-MS). (D) Myobong Formation from the Dongjeom section (DJ-MB). Opaque minerals in (B) and (D) are ilmenite.

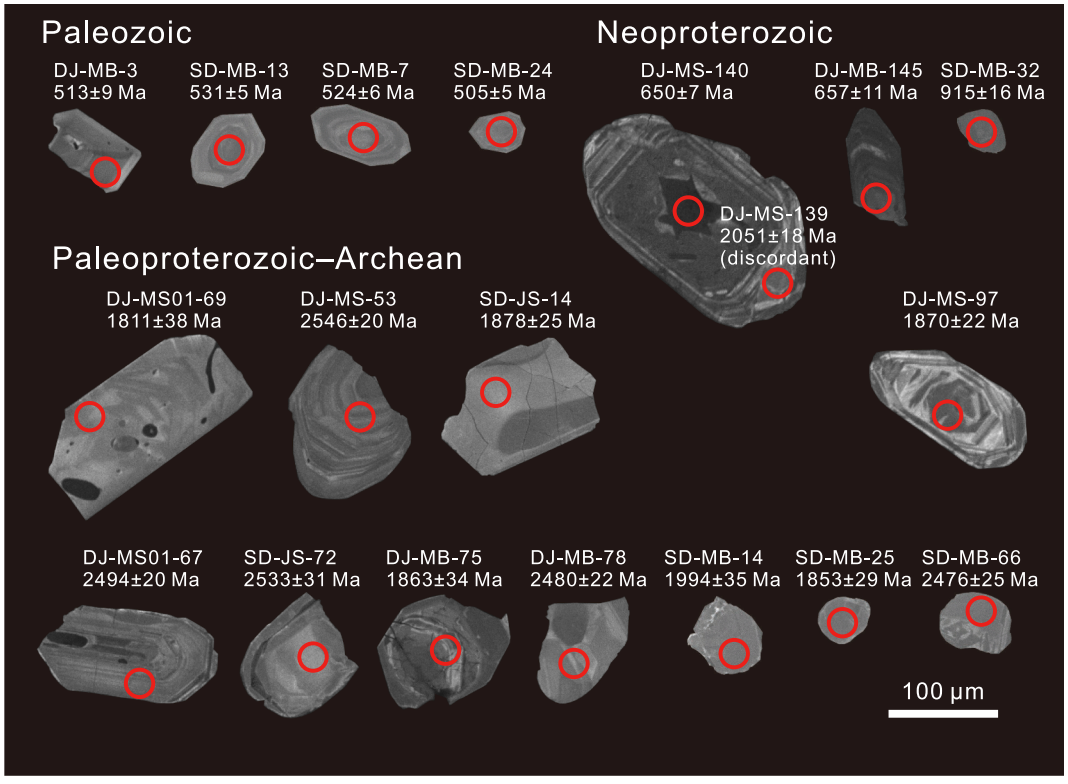

Fig. 8. Representative scanning-electron-microscope cathodoluminescence images of detrital zircon analyzed in this study. Red circles are the analysis spots (25 μm in diameter). Spot numbers are shown together with the $^{206}Pb/^{238}U$ and $^{207}Pb/^{206}Pb$ ages for zircon younger and older than 1000 Ma, respectively. (For interpretation of the references to colour in this figure legend, the reader is referred to the web version of this article.)

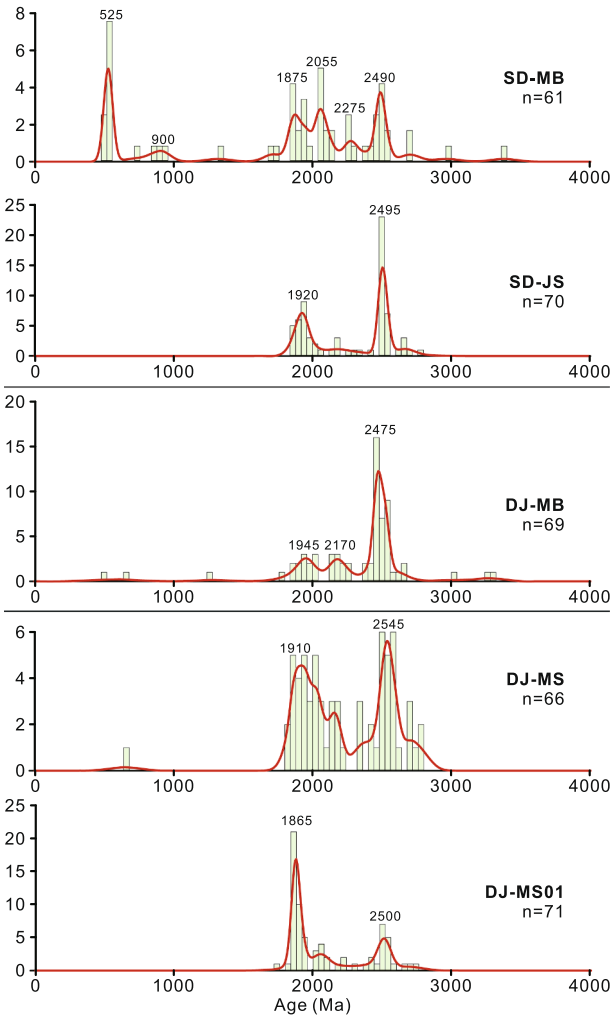

Fig. 9. Kernel density estimates (Vermeesch, 2013) of detrital zircon U–Pb ages from sandstone in the Jangsan (SD-JS) and Myobong (SD-MB and DJ-MB) formations and quartzite clasts in the Myeonsan Formation (DJ-MS and DJ-MS01). The curves were conducted from the $^{206}Pb/^{238}U$ and $^{207}Pb/^{206}Pb$ ages (discordance <10%) for zircon younger and older than 1000 Ma, respectively. For sample locations, see Fig. 2. For raw data, see Supplementary Table 1.

zircon (Fig. 8) yielded 130 concordant ages from samples SD-MB and DJ-MB (Fig. 9; Supplementary Table 1). The two samples show different zircon age spectra. The age population of DJ-MB mostly consists of Paleoproterozoic (64%) and Archean (32%) ages, with peaks at 1945, 2170, and 2475 Ma. The detrital zircon age spectrum of SD-MB mainly comprises Paleozoic (15%), Neoproterozoic (12%), Paleoproterozoic (59%), and Archean (13%) ages, with major age peaks at 525, 900, 1875, 2055, 2275, and 2490 Ma. Such a variety of zircon age groups, including early Paleozoic and Neoproterozoic, was detected only in SD-MB among the samples analyzed in this study. The zircon age spectra of both Myobong Formation samples are also different from those of the Seokgaejae section, which has yielded early Paleozoic, Neoproterozoic, and Mesoproterozoic age groups (Y.I. Lee et al., 2012, 2016c; Cho et al., 2021), indicating spatial and/or temporal heterogeneity of the source rocks of the Myobong Formation.

5.3. Clasts of the Myeonsan Formation

A total of 137 concordant zircon ages was obtained from two sandstone clasts (samples DJ-MS and DJ-MS01) of the lowermost Myeonsan Formation (Fig. 8; Supplementary Table 1). Each clast yielded slightly different zircon age spectra. The zircon age distribution of DJ-MS01 (71 zircon) consists of Paleoproterozoic (82%) and Archean (18%) ages (Fig. 9). The most prominent age peak occurs at 1865 Ma, followed by 2500 Ma. DJ-MS (66 zircon) includes zircon grains with Paleoproterozoic (67%) and Archean (32%) formation ages with one Neoproterozoic-aged zircon (650 ± 7 Ma) (Fig. 9). The youngest age of 443 ± 9 Ma is not dealt with in this study for the same reason as the SD-JS. The age groups between two major peaks at 1910 and 2545 Ma. The age spectrum of both samples is comparable to that of the Jangsan Formation (Y.I. Lee et al., 2012, 2016c; S.W. Kim et al., 2017; H.S. Kim et al., 2019; Cho et al., 2021) and DJ-MB in this study.

6. Discussion

6.1. Depositional age of the Jangsan and Myobong formations

6.1.1. Sedimentary petrological evidence

The outcrop and thin-section observations suggest that the Jangsan–Myobong boundary in the Sangdong section has not been affected by post-depositional tectonic events, in contrast to the west Dongjeom section containing a fault-bounded contact (Chough et al., 2016) that might have formed during the Cretaceous. The sharp boundary between the Jangsan and Myobong formations in the Sangdong section (Fig. 3A), the abrupt changes in lithology across the formation boundary (Fig. 3B, C), and the occurrence of sandstone clasts in the overlying Myobong Formation that might have been derived from the underlying Jangsan Formation (Figs. 3D, 5) collectively suggest that these two formations have an unconformable relationship. The absence of pre-Myobong sandstone in the geographically adjacent area except for the Jangsan Formation, which could have been source of these sandstone clasts, supports this interpretation (Fig. 1) (GICTR, 1962). The Jangsan Formation sometimes contains clasts, but these are mostly quartzite or metasedimentary rocks in composition without sandstone clast (Son and Cheong, 1965; Kobayashi, 1966; J. Kim and Y.I. Lee, 2006; Woo et al., 2006).

In the east Dongjeom and Seokgaejae sections, the coarse sandstone of the Myeonsan Formation are intercalated with mudstone and siltstone in the upper part, and the succession gradually changes into the Myobong Formation (Fig. 2) (Kwon et al., 2006; Woo et al., 2006). This pattern is similar with that of the Myobong Formation in the Sangdong section, where the complete sedimentological log of the Myobong Formation was drawn (Oh, 2020). In the Sangdong section, the Myobong Formation is divided into four units: immature sandstone/conglomerate; lenticular bedded sandstone with stromatolites; siltstone and sandstone representing a tidal rhythmite deposit; and bioturbated sandstone in ascending order (Oh, 2020). Of these, the lowermost sandstone/conglomerate unit is very similar to the Myeonsan Formation in grain size, and in containing abundant detrital ilmenite grains and sandstone clasts, although the unit lacks basal conglomerate (J.Y. Kim, 1991; H.S. Kim et al., 2013). Abundant detrital ilmenite grains in the basal Myobong Formation in the Sangdong section as well as the Myeonsan Formation can be interpreted as paleoplacer deposits formed on the sub-Cambrian surface (Y.I. Lee et al., 2016b) that resulted from intensive weathering of the Precambrian basement rocks (Parnell et al., 2014). The upper three units are generally fine-grained and are superficially similar to the “shales” of the Myobong Formation in other areas that are underlain by the Myeonsan Formation. Together with the complete absence of detrital ilmenite in the Jangsan Formation (Son and Cheong, 1965; Kobayashi, 1966; J. Kim and Y.I. Lee, 2006; Woo et al., 2006), these collectively suggest that the basal Myobong Formation in the Sangdong section and the Myeonsan Formation in Dongjeom and Seokgaejae sections can be in fact lateral equivalents.

6.1.2. Paleontological consideration

The Cambrian Explosion resulted in a complete turnover in the sedimentary system: shelly fossils began to be incorporated into rocks, and organisms began to dig into soft sediments, resulting in the

Cambrian Substrate Revolution (Seilacher, 1999; Mángano and Buatois, 2017). In contrast to well-preserved sedimentary structures in Precambrian sedimentary rocks, Phanerozoic sedimentary rocks are commonly bioturbated, leading to the appearance of a mixed layer that was homogenized by bioturbation (Droser and Bottjer, 1988; Bottjer et al., 2000; Droser and Li, 2001; Álvaro et al., 2013; Tarhan et al., 2015; Gougeon et al., 2018). Calcareous skeletons of organisms became a major part of the carbonate facies (Pruss et al., 2010) as various shelly fossils evolved as part of the Cambrian Explosion (Tucker, 1992; Knoll, 2003).

The age of the Jangsan Formation is uncertain due to the complete absence of fossils (Kobayashi, 1966). It is possible that fossils are not preserved in the "mature" quartzose sandstone of the Jangsan Formation; however, Cambrian quartzose sandstone elsewhere in the world often contain ichnofossils such as *Skolithos*, and are commonly called piperock (Hallam and Swett, 1966; Peterson and Clark, 1974; Droser, 1991; Khalifa et al., 2006; Desjardins et al., 2010). Nonetheless, the absence of fossils cannot be solid evidence to assign a Precambrian age to a formation. The Myeonsan Formation is also known to be unfossiliferous (Woo et al., 2006), but J.Y. Kim (1991) reported the ichnofossils *Skolithos* and *Laevicyclus* from the formation, suggesting that this unit is at least of Phanerozoic age (Bottjer et al., 2000).

There is a consensus on the age of the Myobong Formation, from which trilobites and other fossils have been studied for several decades (Kobayashi, 1935, 1960; H.-Y. Lee et al., 1992). The lowermost biozone of the Myobong Formation contains the trilobite *Redlichia saitoi* (Kobayashi, 1960), and the first appearance datum (FAD) of *Redlichia* has been generally considered to be the base of informal Cambrian Stage 4 (Geyer and Shergold, 2000; Peng et al., 2012; Zhang et al., 2017). Although recent biostratigraphic studies have suggested that the FAD of *Redlichia* can be diachronous (Geyer, 2019), the occurrence of *Redlichia* in the Myobong Formation constrains its age to at least late Cambrian Series 2 (Stage 4). Fossils of *Redlichia* have recently been found in the lower–middle Myobong Formation stratigraphically above the basal sandstone unit, geographically adjacent to Kobayashi (1960)'s locality (ca. 4 km southwest of the Dongjeom section) (Lee, S.-b., per. comm.).

6.1.3. Detrital zircon geochronological consideration

The detrital zircon samples were collected in order to estimate depositional ages of the Jangsan and Myobong formations, and to understand how rapid the provenance change across the Jangsan–Myobong boundary reported by Y.I. Lee et al. (2016c) was. The detrital zircon from the Jangsan Formation commonly show bimodal peaks at ca. 1900 and 2500 Ma, and there is no zircon younger than 1738 ± 67 Ma (the youngest zircon age of 1630 ± 141 Ma reported by Cho et al. (2021) is not considered because of its large error range) (Fig. 10) (Y.I. Lee et al., 2012, 2016c; S.W. Kim et al., 2017; H.S. Kim et al., 2019; Cho et al., 2021; C. Lee et al., in press; this study). These ages are very similar to those of the basement rocks of the Sino-Korean Block (Darby and Gehrels, 2006). The Jangsan Formation was thought to have been deposited after the Paleoproterozoic, based on its youngest zircon age (Y.I. Lee et al., 2012) and its stratigraphic position overlying the Paleoproterozoic Yuli Group (Y.I. Lee et al., 2011; Jeong, 2020), and prior to the deposition of the Myobong Formation (Cambrian Series 2; Stage 4), between 1800 and 520 Ma. Correlatable sedimentary rocks in eastern North China were deposited throughout the late Paleo- to Neoproterozoic (Meng et al., 2011; Zuo et al., 2019), but these rocks are characterized by variable detrital zircon age spectra. The detrital zircon age spectra of Mesoproterozoic sedimentary rocks in the eastern (Liu et al., 2013), north-central, and southern (Li et al., 2020c) parts of the Sino-Korean Block are all characterized by dominant Paleoproterozoic and Archean-aged zircon with bimodal peaks at around 1800 and 2600 Ma, and are generally comparable to those of the Jangsan Formation. Similarly, Neoproterozoic successions north of Beijing (Wan et al., 2011) and in the southern Sino-Korean Block (Li et al., 2020b) contain 2600–1800-Ma detrital zircon, without any younger than 1600 Ma. In contrast, Neoproterozoic sedimentary rocks in the eastern Sino-Korean Block (Shandong and Liaoning provinces of China, and North Korea) contain many Meso- and Neoproterozoic-aged zircon that may record the breakup of Rodinia and formation of rift basins in the Sino-Korean Block (Hu et al., 2012; He et al., 2017; Wan et al., 2019). These comparisons suggest that detrital zircon data alone cannot further constrain the depositional age of the Jangsan Formation, and other methods are required to understand its stratigraphic implications.

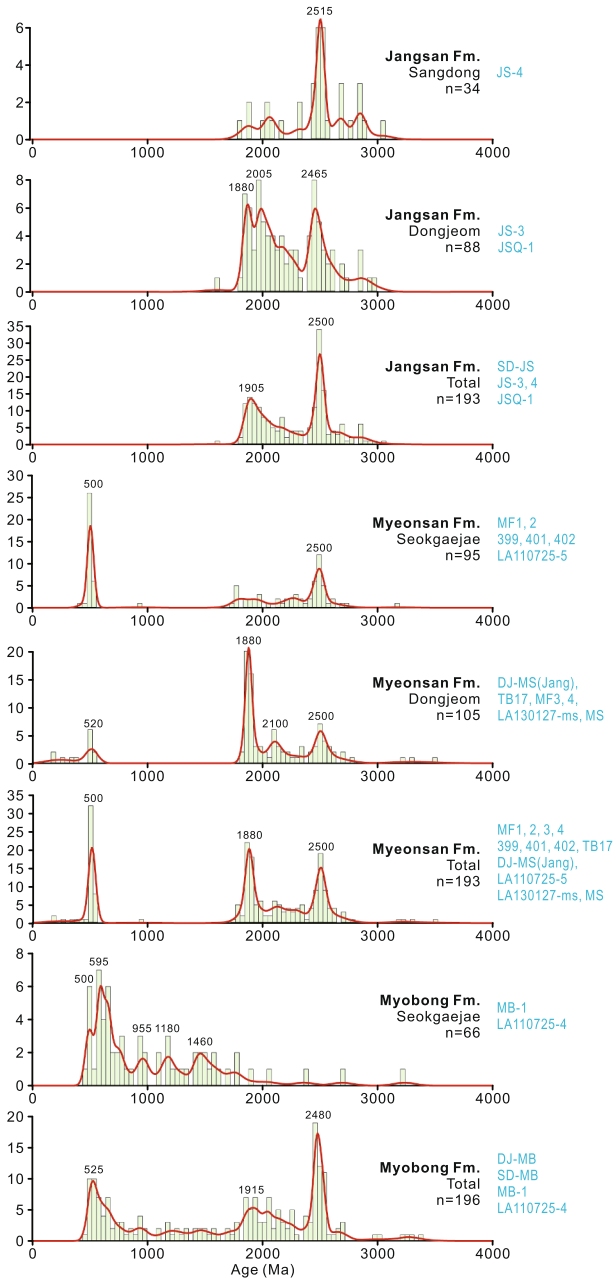

Fig. 10. Kernel density estimates of detrital zircon U–Pb ages of the Jangsan, Myeonsan, and Myobong formations using data compiled from previous studies and this study (marked in blue). The compiled data are the $^{206}Pb/^{238}U$ and $^{207}Pb/^{206}Pb$ ages (discordance <10%) for zircon younger and older than 1000 Ma, respectively. For sample names and locations, see Fig. 2. (For interpretation of the references to colour in this figure legend, the reader is referred to the web version of this article.)

In contrast, the Myobong Formation has different detrital zircon age populations in different places, as described above (see also Fig. 9), but all populations commonly contain Cambrian- to Neoproterozoic-aged

zircon (Fig. 10) (Y.I. Lee et al., 2012; Jang et al., 2018; H.S. Kim et al., 2019; Cho et al., 2021; this study). The diverse detrital zircon age spectra of the Myobong Formation may record temporal and areal changes in sedimentation patterns during the early transgression. The basal Myobong sandstone (and correlatable Myeonsan sandstone) would have been deposited in the early stage of the transgression. Their zircon age populations commonly comprise Cambrian and Paleoproterozoic–Archean ages (Figs. 9, 10); these sediments could have been supplied from the adjacent basement rocks of Paleoproterozoic–Archean age (H.S. Kim et al., 2019) and some newly generated sediments from the early Paleozoic magmatic arc that might have existed at the margin of Sino-Korean Block (Cho et al., 2021). The subsequent rapid transgression during the deposition of the Myobong Formation would have imported Cambrian- and Neoproterozoic-aged zircon from a much further source on the Gondwana mainland (Fig. 10) (H.S. Kim et al., 2019).

The statistical similarity of the detrital zircon age distributions of the Jangsan, Myeonsan, and Myobong formations obtained in this and previous studies (Y.I. Lee et al., 2012, 2016c; H.S. Kim et al., 2013; S.W. Kim et al., 2017; Jang et al., 2018; Cho et al., 2021; this study) is compared on a multi-dimensional scaling map (Fig. 11) (Vermeesch et al., 2016). In this map, samples with similar age spectra are arranged closer together compared with samples with dissimilar spectra. The zircon age distributions of the two clasts from the Myeonsan Formation (DJ-MS and DJ-MS01) are located closer to the samples from the Jangsan and Myeonsan formations than the other samples. DJ-MS is the closest sample to SD-JS in this map, while DJ-MS01 is most similar to the zircon age spectra of the Myeonsan Formation in the Dongjeom section (Figs. 9–11). This suggests that the clast DJ-MS01 could have been derived from a source rock of the Myeonsan sandstone other than the Jangsan Formation. However, considering the absence of the Precambrian sandstone in the adjacent basement rocks (Fig. 1) (GICTR, 1962) and heterogeneity of the detrital zircon age population of the Jangsan Formation (Y.I. Lee et al., 2012), both of these sandstone clasts can be grouped with the Jangsan sandstone.

In addition, the abrupt change in detrital zircon age population across the Jangsan–Myobong formation boundary in the Sangdong section (Fig. 9) suggests that there is either an unconformity across the boundary (Y.I. Lee et al., 2012) or that there was an abrupt change in sediment provenance (H.S. Kim et al., 2019). In this study, this abrupt change was detected within stratigraphically adjacent intervals, just 1 m apart, that are similar in grain size (Fig. 3A). Thus, the complete absence of Cambrian- and Neoproterozoic-aged zircon in the Jangsan sandstone, in contrast to their abundance in the Myobong sandstone, cannot be easily explained by a provenance shift. Together with sedimentary petrological evidence, the detrital zircon geochronology supports the existence of the Great Unconformity between the Jangsan and Myobong formations. The duration of the Great Unconformity on the Sino-Korean Block is uncertain. However, the rarity of Cryogenian–early Cambrian (Terreneuvian) sedimentary rocks throughout the block (He et al., 2017) suggests that the Jangsan Formation is likely to be older than the Tonian.

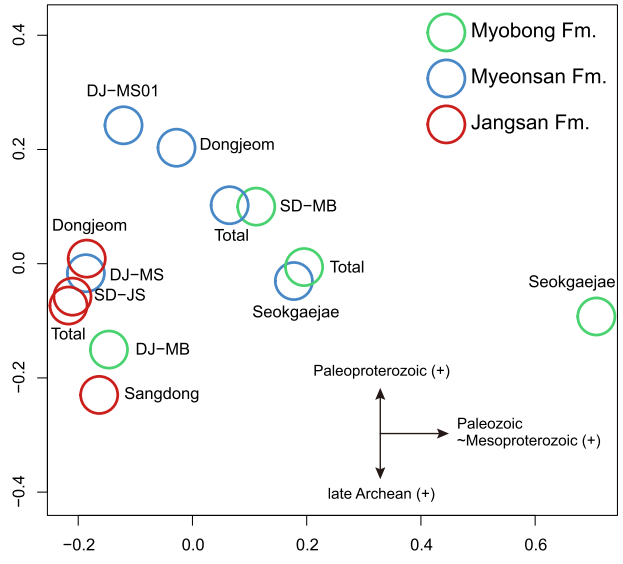

Fig. 11. Multidimensional scaling (Vermeesch et al., 2016) map of detrital zircon ages of the Jangsan, Myeonsan, and Myobong formations (using the same data as Figs. 9 and 10). The arrows indicate the trends of increasing age population.

6.2. *The Great Unconformity in the Sino-Korean Block*

6.2.1. *Reconsideration of regional stratigraphy*

The stratigraphy of the Taebaek Group was first proposed by Kobayashi (1930, 1935, 1966). According to this classification, the lower part of the group consists only of the Jangsan and Myobong formations, the view followed by GICTR (1962) and Cheong (1969). The Myeonsan Formation was erected by Cheong et al. (1973) for the basal conglomerate and coarse sandstone in the Dongjeom section, which was considered to be a lateral equivalent of the Jangsan Formation (J.Y. Kim and Cheong, 1987). This view was subsequently followed by various researchers (Y.I. Lee and J.I. Lee, 2003; Kwon et al., 2006; Woo et al., 2006). The occurrence of two contrasting lithologic units is interpreted as a result of local subsidence during the initial transgression (Woo et al., 2006).

However, petrographic similarity between the basal Myobong Formation in the Sangdong section and the Myeonsan Formation in the east of the Dongjeom Fault suggests that these two units can be lithostratigraphically comparable (Fig. 2). We propose that these coarse-grained units are lateral equivalents, and regional stratigraphy needs to be refined accordingly. The Myeonsan and Myobong formations would have been deposited on top of basement rocks (Jangsan Formation, Yuli Group and Hongjesa granite) via a disconformity or nonconformity. The Jangsan and Myobong formations are generally parallel to one another, and this boundary can be traced up to 80 km southwest in the Danyang area (GICTR, 1962; H.S. Kim et al., 2019). Such a lithologic uniformity along the Jangsan–Myobong boundary, although the boundary itself is often fault-bounded (Chough et al., 2016; Uhmb, 2018), indicates the wide extent of the unconformity. Finding more outcrops bearing the Jangsan–Myobong boundary as well as the entire Myobong Formation will be helpful to clarify stratigraphy of the basal Taebaek Group.

6.2.2. *Paleogeographic implications of the Great Unconformity*

The lower Paleozoic sedimentary rocks of the Taebaeksan Basin have historically been compared well with those in various parts of North China and the Pyeongnam Basin of North Korea (e.g., Kobayashi, 1930, 1966; Chough et al., 2000; Kwon et al., 2006; Chough, 2013), in terms of biostratigraphy (Choi et al., 2016 and references therein), paleobiogeography (Jeong and Y.I. Lee, 2000, 2004; S.-b. Lee et al., 2008; Choi and Park, 2017), sequence stratigraphy (Kwon et al., 2006; Chen et al., 2012), and lithostratigraphy (Chough et al., 2010). The sedimentation pattern on the Sino-Korean Block was generally similar throughout geologic time, before its collision with South China Block during the Permian–Triassic. Sedimentation began on the craton in the late Paleoproterozoic (ca. 1.6 Ga?), and lasted until the Neoproterozoic (Sinian) (Meng et al., 2011; Zuo et al., 2019). These Precambrian sedimentary rocks are unconformably overlain by Cambrian–Ordovician sedimentary rocks via the Great Unconformity (Meng et al., 1997). Sedimentation ceased in the Middle–Late Ordovician, resulting in the platform-wide hiatus of the "Great Hiatus" (D.-C. Lee et al., 2017) or the Huaiyuan Epeirogeny (Zhen et al., 2016) that lasted until the early Carboniferous.

In addition to the newly proposed Precambrian–Cambrian disconformity in the Taebaeksan Basin, similar unconformities are found

throughout the Sino-Korean Block over a distance of 2000 km, especially along the marginal areas of the block, including the western (Fig. 12A, B; Subaigou section, Inner Mongolia Province; Zhang et al., 2020), southwestern (Shuiyougou section, Shanxi Province; Luonan section, Shaanxi Province; Xiao et al., 1997), southeastern (Fig. 12C, D; Liangcheong section, Shandong Province; Chough et al., 2010; Dalian region, Liaoning Province; He et al., 2017; Huaibei region, Anhui Province; Wan et al., 2019), and north-central (Fig. 12E, F; Western Hill section, Beijing; Meng et al., 1997; Jixian section, Tianjin; Xiao et al., 1997) areas as well as the Pyeongnam Basin of North Korea (Zhai et al., 2019). All of these Cambrian sedimentary rocks disconformably overlie Neoproterozoic (Shanxi, Shaanxi, Anhui, Liaoning, Shandong provinces, the Beijing and Tianjin areas, and North Korea) or Mesoproterozoic (Inner Mongolia Province) sedimentary rocks. This consistency suggests that the Great Unconformity on the Sino-Korean Block mainly developed as a disconformable boundary, and this disconformity might have been extended to the Taebaek area. It further emphasizes the importance of eustatic control on the formation of the boundary in addition to the local tectonics; e.g., the assembly of Gondwana (Brasier and Lindsay, 2001; Meert and Lieberman, 2008; Keller et al., 2019; Shahkarami et al., 2020).

7. Conclusions

The Jangsan Formation, previously considered to be the basal Cambrian deposit of the lower Paleozoic Joseon Supergroup in the eastern Korean Peninsula, could be Precambrian in age. The disconformity separating the Jangsan Formation from the overlying Cambrian Myobong Formation is interpreted to represent the Great Unconformity. The Myeonsan Formation, which has traditionally been considered to be a lateral equivalent of the Jangsan Formation, is correlated with the basal part of the Myobong Formation. Although limited outcrop exposure, as well as fault-bounded Jangsan–Myobong boundary elsewhere, hinder understanding of the stratigraphic relationships between these lithostratigraphic units, further studies including detailed mapping, sedimentary facies analysis and correlation, and biostratigraphic analysis would help to further elucidate their nature.

CRediT authorship contribution statement

Jeong-Hyun Lee: Conceptualization, Formal analysis, Data curation. **Min-Kyu Oh:** Data curation. **Taejin Choi:** Conceptualization, Formal analysis.

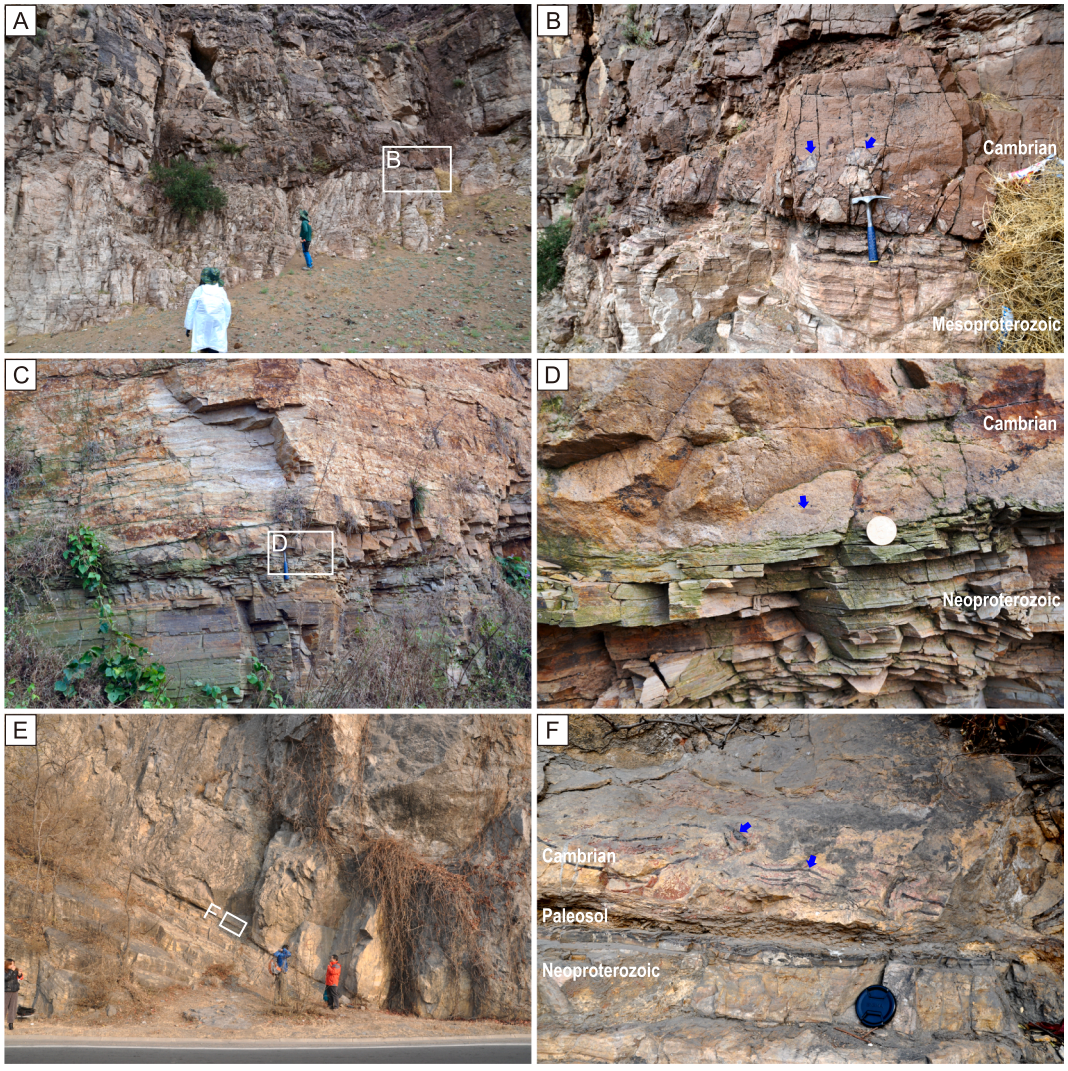

Fig. 12. The Precambrian–Cambrian boundary in other areas of the Sino-Korean Block. (A, B) Subaigou section, Wuhai, Inner Mongolia (39°40′11″N 106°56′50″E). (B) Arrows point to reworked Mesoproterozoic sandstone clasts. Hammer for scale in (B) and (C) is 27 cm long. (C, D) Liangcheong section, Linyi, Shandong Province (34°56′29″N 118°06′34″E) (see Chough et al., 2010, figs. 4c, 7). (D) Arrow points to mudstone clast originating from the underling strata. Coin for scale is 20.5 mm in diameter. (E, F) Western Hill section, Beijing (40°00′23″N 116°01′46″E). (F) Arrows point to mudstone clasts derived from the underlying Precambrian strata. Lens cap for scale in (F) is 7.2 cm in diameter. For locations, see Fig. 1A.

Declaration of Competing Interest

The authors declare that they have no known competing financial interests or personal relationships that could have appeared to influence the work reported in this paper.

Acknowledgments

We thank S.K. Chough, Y.I. Lee, D.-J. Lee, S.-J. Choh, Y.K. Kwon, H.S. Lee, J. Woo, and S.H. Cho for discussion of the Jangsan and Myeonsan formations, S.-b. Lee for finding trilobites from the Myobong Formation, and T. Nærra (Lund University) for analysis of detrital zircon. We are very grateful to J. Hagadorn and two anonymous reviewers for helpful comments, and to N. Wodicka for expert editorial guidance. This study was supported by National Research Foundation of Korea grants to JHL (2019R1A2C4069278) and to TC (2020R111A3072160).

Appendix A. Supplementary data

Supplementary data to this article can be found online at https://doi.org/10.1016/j.precamres.2021.106363.

References

Álvaro, J.J., Zamora, S., Clausen, S., Vizcaïno, D., Smith, A.B., 2013. The role of abiotic factors in the Cambrian Substrate Revolution: a review from the benthic community replacements of West Gondwana. Earth Sci. Rev. 118, 69–82. https://doi.org/10.1016/j.earscirev.2013.01.002.

Barnes, M.A., Marshak, S., Zanoni, G., Monson, C.C., Šegvić, B., Sweet, D.E., Pevehouse, K.J., 2020. Paleotopography controls weathering of Cambrian-age profiles beneath the Great Unconformity, St. Francois Mountains, SE Missouri, U.S.A. J. Sediment. Res. 90, 629–650. https://doi.org/10.2110/jsr.2020.33.

Bottjer, D.J., Hagadorn, J.W., Dornbos, S.Q., 2000. The Cambrian substrate revolution. GSA Today 10, 1–7.

Brasier, M.D., Lindsay, J.F., 2001. Did supercontinental amalgamation trigger the "Cambrian explosion"? In: Zhuravlev, A.Y., Riding, R. (Eds.), Ecology of the Cambrian Radiation. Columbia University Press, New York, pp. 69–89.

Chen, J., Chough, S.K., Lee, J.-H., Han, Z., 2012. Sequence-stratigraphic comparison of the upper Cambrian Series 3 to Furongian succession between the Shandong region, China and the Taebaek area, Korea: high variability of bounding surfaces in an epeiric platform. Geosci. J. 16, 357–379. https://doi.org/10.1007/s12303-012-0040-5.

Cheong, C.H., 1969. Stratigraphy and paleontology of the Samcheog Coalfield, Gangweondo, Korea (I). J. Geol. Soc. Korea 5, 13–56.

Cheong, C.H., Lee, D.S., Um, S.H., Chang, K.H., Kim, H.M., 1973. A study to establish the chronostratigraphic units in Korea, Ministry of Science and Technology, pp. 68.

Cho, M., Cheong, W., Ernst, W.G., Kim, Y., Yi, K., 2021. U-Pb detrital zircon ages of Cambrian–Ordovician sandstones from the Taebaeksan Basin, Korea: provenance variability in platform shelf sequences and paleogeographic implications. GSA Bulletin 133, 488–504. https://doi.org/10.1130/b35521.1.

Choi, D.K., 2019. Evolution of the Taebaeksan Basin, Korea: I, early Paleozoic sedimentation in an epeiric sea and break-up of the Sino-Korean Craton from Gondwana. Isl. Arc 28, e12275. https://doi.org/10.1111/iar.12275.

Choi, D.K., Chough, S.K., 2005. The Cambrian-Ordovician stratigraphy of the Taebaeksan Basin, Korea: a review. Geosci. J. 9, 187–214. https://doi.org/10.1007/BF02910579.

Choi, D.K., Chough, S.K., Kwon, Y.K., Lee, S.B., Woo, J., Kang, I., Lee, H.S., Lee, S.M., Sohn, J.W., Shinn, Y.J., Lee, D.J., 2004. Taebaek Group (Cambrian-Ordovician) in the Seokgaejae section, Taebaeksan Basin: a refined Lower Paleozoic stratigraphy in Korea. Geosci. J. 8, 125–151. https://doi.org/10.1007/BF02910190.

Choi, D.K., Lee, J.G., Lee, S.-B., Park, T.-Y.-S., Hong, P.S., 2016. Trilobite Biostratigraphy of the lower Paleozoic (Cambrian–Ordovician) Joseon Supergroup, Taebaeksan Basin, Korea. Acta Geol. Sin. 90, 1976–1999. https://doi.org/10.1111/1755-6724.13016.

Choi, D.K., Park, T.-Y.-S., 2017. Recent advances of trilobite research in Korea: Taxonomy, biostratigraphy, paleogeography, and ontogeny and phylogeny. Geosci. J. 21, 891–911. https://doi.org/10.1007/s12303-017-0041-5.

Chough, S.K., 2013. Geology and Sedimentology of Korean Peninsula. Elsevier Insights, Elsevier, 363 pp. 10.1016/C2012-0-02847-5.

Chough, S.K., Kwon, S.T., Ree, J.-H., Choi, D.K., 2000. Tectonic and sedimentary evolution of the Korean peninsula: a review and new view. Earth Sci. Rev. 52, 175–235. https://doi.org/10.1016/s0012-8252(00)00029-5.

Chough, S.K., Lee, D.J., Ree, J.-H., Choh, S.J., Woo, J., 2016. Comment on "Depositional age and petrological characteristics of the Jangsan Formation in the Taebaeksan Basin, Korea-revisited" by Lee, Y.I., Choi, T. and Lim, H.S. Journal of the Geological Society of Korea 52, 961–967 (in Korean with English abstract). 10.14770/jgsk.2016.52.6.961.

Chough, S.K., Lee, H.S., Woo, J., Chen, J., Choi, D.K., Lee, S.-B., Kang, I., Park, T.-Y., Han, Z., 2010. Cambrian stratigraphy of the North China Platform: revisiting principal sections in Shandong Province, China. Geosci. J. 14, 235–268. https://doi.org/10.1007/s12303-010-0029-x.

Corfu, F., Hanchar, J.M., Hoskin, P.W.O., Kinny, P., 2003. Atlas of zircon textures. Rev. Mineral. Geochem. 53, 469–500. https://doi.org/10.2113/0530469.

Darby, Brian J., Gehrels, George, 2006. Detrital zircon reference for the North China block. J. Asian Earth Sci. 26, 637–648. https://doi.org/10.1016/j.jseaes.2004.12.005.

DeLucia, M.S., Guenthner, W.R., Marshak, S., Thomson, S.N., Ault, A.K., 2018. Thermochronology links denudation of the Great Unconformity surface to the supercontinent cycle and snowball Earth. Geology 46, 167–170. https://doi.org/10.1130/g39525.1.

Desjardins, P.R., Mángano, M.G., Buatois, L.A., Pratt, B.R., 2010. *Skolithos* pipe rock and associated ichnofabrics from the southern Rocky Mountains, Canada: colonization trends and environmental controls in an early Cambrian sand-sheet complex. Lethaia 43, 507–528. https://doi.org/10.1111/j.1502-3931.2009.00214.x.

Droser, M.L., 1991. Ichnofabric of the Paleozoic *Skolithos* ichnofacies and the nature and distribution of *Skolithos* piperock. Palaios 6, 316–325. https://doi.org/10.2307/3514911.

Droser, M.L., Bottjer, D.J., 1988. Trends in depth and extent of bioturbation in Cambrian carbonate marine environments, western United States. Geology 16, 233–236. https://doi.org/10.1130/0091-7613(1988)016<0233:TIDAEO>2.3.CO;2.

Droser, M.L., Li, X., 2001. The Cambrian radiation and the diversification of sedimentary fabrics. In: Zhuravlev, A.Y., Riding, R. (Eds.), Ecology of the Cambrian Radiation. Columbia University Press, New York, pp. 137–169.

Geological Investigation Corps of Taebaeksan Region (GICTR), 1962. Report on the Geology and Mineral Resources of the Taebaegsan Region. Geological Society of Korea, Seoul, 89 pp (in Korean).

Geyer, G., 2019. A comprehensive Cambrian correlation chart. Episodes 42, 321–332. https://doi.org/10.18814/epiiugs/2019/019026.

Geyer, G., Shergold, J., 2000. The quest for internationally recognized divisions of Cambrian time. Episodes 23, 188–195. https://doi.org/10.18814/epiiugs/2000/v23i3/006.

Gougeon, R.C., Mangano, M.G., Buatois, L.A., Narbonne, G.M., Laing, B.A., 2018. Early Cambrian origin of the shelf sediment mixed layer. Nat. Commun. 9, 1909. https://doi.org/10.1038/s41467-018-04311-8.

Hallam, A., Swett, K., 1966. Trace fossils from the Lower Cambrian Pipe Rock of the north-west Highlands. Scott. J. Geol. 2, 101–106. https://doi.org/10.1144/sjg02010101.

Han, Y., Zhao, G., Cawood, P.A., Sun, M., Eizenhöfer, P.R., Hou, W., Zhang, X., Liu, Q., 2016. Tarim and North China cratons linked to northern Gondwana through switching accretionary tectonics and collisional orogenesis. Geology 44, 95–98. https://doi.org/10.1130/g37399.1.

He, T., Zhou, Y., Vermeesch, P., Rittner, M., Miao, L., Zhu, M., Carter, A., Pogge von Strandmann, P.A.E., Shields, G.A., 2017. Measuring the 'Great Unconformity' on the North China Craton using new detrital zircon age data. In: Brasier, A.T., McIlroy, D., McLoughlin, N. (Eds.), Earth System Evolution and Early Life: a Celebration of the Work of Martin Brasier, 448. Geological Society of London Special Publications, pp. 145–159. https://doi.org/10.1144/sp448.14.

Hu, B., Zhai, M., Li, T., Li, Z., Peng, P., Guo, J., Kusky, T.M., 2012. Mesoproterozoic magmatic events in the eastern North China Craton and their tectonic implications: Geochronological evidence from detrital zircons in the Shandong Peninsula and North Korea. Gondwana Res. 22, 828–842. https://doi.org/10.1016/j.gr.2012.03.005.

Jackson, S.E., Pearson, N.J., Griffin, W.L., Belousova, E.A., 2004. The application of laser ablation-inductively coupled plasma-mass spectrometry to in situ U-Pb zircon geochronology. Chem. Geol. 211, 47–69. https://doi.org/10.1016/j.chemgeo.2004.06.017.

Jang, Y., Kwon, S., Song, Y., Kim, S.W., Kwon, Y.K., Yi, K., 2018. Phanerozoic polyphase orogenies recorded in the northeastern Okcheon Belt, Korea from SHRIMP U-Pb detrital zircon and K-Ar illite geochronologies. J. Asian Earth Sci. 157, 198–217. https://doi.org/10.1016/j.jseaes.2017.08.002.

Jeong, H., Lee, Y.I., 2000. Late Cambrian biogeography: conodont bioprovinces from Korea. Palaeogeogr. Palaeoclimatol. Palaeoecol. 162, 119–136. https://doi.org/10.1016/S0031-0182(00)00108-5.

Jeong, H., Lee, Y.I., 2004. Nd isotopic study of Upper Cambrian conodonts from Korea and implications for early Paleozoic paleogeography. Palaeogeogr. Palaeoclimatol. Palaeoecol. 212, 77–94. https://doi.org/10.1016/j.palaeo.2004.05.018.

Jeong, S.W., 2020. Timing of deposition of the Yuli Group distributed in the Northeastern Yeongnam Massif constrained by zircon and monazite U-Pb ages. M.S. Thesis. Pukyong National University, 87 pp.

Karlstrom, K., Hagadorn, J., Gehrels, G., Matthews, W., Schmitz, M., Madronich, L., Mulder, J., Pecha, M., Giesler, D., Crossey, L., 2018. Cambrian Sauk transgression in the Grand Canyon region redefined by detrital zircons. Nat. Geosci. 11, 438–443. https://doi.org/10.1038/s41561-018-0131-7.

Keller, C.B., Husson, J.M., Mitchell, R.N., Bottke, W.F., Gernon, T.M., Boehnke, P., Bell, E.A., Swanson-Hysell, N.L., Peters, S.E., 2019. Neoproterozoic glacial origin of the Great Unconformity. Proc. Natl. Acad. Sci. 116, 1136–1145. https://doi.org/10.1073/pnas.1804350116.

Khalifa, M.A., Soliman, H.E., Wanas, H.A., 2006. The Cambrian Araba Formation in northeastern Egypt: Facies and depositional environments. J. Asian Earth Sci. 27, 873–884. https://doi.org/10.1016/j.jseaes.2005.09.003.

Kim, H.S., Choh, S.-J., Lee, J.-H., Kim, S.J., 2019. Sediment grain size does matter: implications of spatiotemporal variations in detrital zircon provenance for early Paleozoic peri-Gondwana reconstructions. Int. J. Earth Sci. 108, 1509–1526. https://doi.org/10.1007/s00531-019-01717-7.

Kim, H.S., Hwang, M.-K., Ree, J.-H., Yi, K., 2013. Tectonic linkage between the Korean Peninsula and mainland Asia in the Cambrian: insights from U-Pb dating of detrital zircon. Earth Planet. Sci. Lett. 368, 204–218. https://doi.org/10.1016/j.epsl.2013.03.003.

Kim, J.H., Yoon, W.S., Choi, J.W., Kwon, H.S., Bae, G.H., Cheong, S.W., 2000. Geological structures in the Tongri-Dogye and Sangdeog areas in the eastern part of the Samcheog Coalfield, Korea. Geosci. J. 4, 153–163. https://doi.org/10.1007/BF02910134.

Kim, J.Y., 1991. Stratigraphy of the Myeonsan Formation in Samcheoggun, Kangwondo and Ponghwagun, Kyongsangbukdo. J. Geol. Soc. Korea 27, 225–245.

Kim, J.Y., Cheong, C.H., 1987. The Precambrian-Cambrian boundary in the east of the Dongjeom Fault, Gangweon-do, Korea. J. Geol. Soc. Korea 23, 145–158.

Kim, S.W., Park, S.-I., Jang, Y., Kwon, S., Kim, S.J., Santosh, M., 2017. Tracking Paleozoic evolution of the South Korean Peninsula from detrital zircon records: implications for the tectonic history of East Asia. Gondwana Res. 50, 195–215. https://doi.org/10.1016/j.gr.2017.05.009.

Kim, Y., Lee, Y.I., 2006. Early evolution of the Duwibong Unit of the lower Paleozoic Joseon Supergroup, Korea: a new view. Geosci. J. 10, 391–402. https://doi.org/10.1007/BF02910434.

Knoll, A.H., 2003. Biomineralization and evolutionary history. Rev. Mineral. Geochem. 54, 329–356. https://doi.org/10.2113/0540329.

Kobayashi, T., 1930. Cambrian and Ordovician faunas of South Korea and the bearing of the Tsinling-Keijo Line on Ordovician palaeogeography. In: Proceedings of the Imperial Academy of Tokyo VI, pp. 423–426.

Kobayashi, T., 1935. The Cambro-Ordovician formations and faunas of South Chosen, Paleontology, Part III, Cambrian faunas of South Chosen with a special study on the Cambrian trilobite genera and families. J. Faculty Sci., Imperial Univ. Tokyo, Section II 4, 49–344.

Kobayashi, T., 1960. The Cambro-Ordovician formations and faunas of South Chosen, Palaeontology, Part VII, Palaeontology VI, Supplement to the Cambrian Faunas of the Tsuibon Zone with notes on some Trilobites genera and families. J. Faculty Sci., Univ. Tokyo, Section II 7, 329–420.

Kobayashi, T., 1966. The Cambro-Ordovician formations and faunas of South Korea, Part X, Stratigraphy of the Chosen Group in Korea and South Manchuria and its relation to the Cambro-Ordovician formations of other areas, Section A. The Chosen Group of South Korea. J. Faculty Sci., Univ. Tokyo, Section II 16, 1–84.

Kwon, Y.K., Chough, S.K., Choi, D.K., Lee, D.J., 2006. Sequence stratigraphy of the Taebaek Group (Cambrian-Ordovician), mideast Korea. Sed. Geol. 192, 19–55. https://doi.org/10.1016/j.sedgeo.2006.03.024.

Lee, C., Kwon, Y.K., Yeo, J.M., Kwon, Y.J., Han, H.-C., in press. U-Pb ages of detrital zircons in lower Palaeozoic quartzites of the Taebaeksan Basin, eastern Sino–Korean Block: sediment provenance response to relative sea-level changes. Int. Geol. Rev., 10.1080/00206814.2020.1827304.

Lee, D.-C., Choh, S.-J., Lee, D.-J., Ree, J.-H., Lee, J.-H., Lee, S.-B., 2017. Where art thou "the great hiatus?" – review of Late Ordovician to Devonian fossil-bearing strata in the Korean Peninsula and its tectonostratigraphic implications. Geosci. J. 21, 913–931. https://doi.org/10.1007/s12303-017-0046-0.

Lee, H.-S., Park, K.-H., Song, Y.-S., Kim, N.-H., Orihashi, Y., 2010. LA-ICP-MS U-Pb zircon age of the Hongjesa Granite in the northeast Yeongnam Massif. J. Petrol. Soc. Korea 19, 103–108 (in Korean with English abstract).

Lee, H.-Y., Roh, D.-S., Lee, B.-S., Yi, M.-S., 1992. Small shelly fossils and conodonts from the Myobong and Daegi formations in Baegunsan Syncline, Yeongweol-Jeongseon area, Kangweon-do. J. Paleontol. Soc. Korea 8, 140–163.

Lee, J.-H., Hong, J., Woo, J., Oh, J.-R., Lee, D.-J., Choh, S.-J., 2016a. Reefs in the early Paleozoic Taebaek Group, Korea: a review. Acta Geol. Sin. 90, 352–367. https://doi.org/10.1111/1755-6724.12659.

Lee, S.-B., Lee, D.-C., Choi, D.K., 2008. Cambrian-Ordovician trilobite family Missisquoiidae Hupé, 1955: systematic revision and palaeogeographical considerations based on cladistic analysis. Palaeogeogr. Palaeoclimatol. Palaeoecol. 260, 315–341. https://doi.org/10.1016/j.palaeo.2007.11.008.

Lee, Y.I., Choi, T., Lim, H.S., 2016b. Depositional age and petrological characteristics of the Jangsan Formation in the Taebaeksan Basin, Korea-revisited. J. Geol. Soc. Korea 52, 67–77 (in Korean with English abstract). 10.14770/jgsk.2016.52.1.67.

Lee, Y.I., Choi, T., Lim, H.S., Orihashi, Y., 2012. Detrital zircon U-Pb ages of the Jangsan Formation in the northeastern Okcheon belt, Korea and its implications for material source, provenance, and tectonic setting. Sed. Geol. 282, 256–267. https://doi.org/10.1016/j.sedgeo.2012.09.005.

Lee, Y.I., Choi, T., Lim, H.S., Orihashi, Y., 2016c. Detrital zircon geochronology and Nd isotope geochemistry of the basal succession of the Taebaeksan Basin, South Korea: Implications for the Gondwana linkage of the Sino-Korean (North China) block during the Neoproterozoic–early Cambrian. Palaeogeogr. Palaeoclimatol. Palaeoecol. 441, 770–786. https://doi.org/10.1016/j.palaeo.2015.10.025.

Lee, Y.I., Choi, T., Orihashi, Y., 2011. LA-ICP-MS zircon U-Pb ages of the Precambrian Yuli Group. J. Geol. Soc. Korea 47, 81–87 (in Korean).

Lee, Y.I., Lee, J.I., 2003. Paleozoic sedimentation and tectonics in Korea: a review. Island Arc 12, 162–179. https://doi.org/10.1046/j.1440-1738.2003.00388.x.

Li, G., Chen, L., Pang, K., Zhou, G., Han, C., Yang, L., Lv, W., Wu, C., Wang, W., Yang, F., 2020a. An assemblage of macroscopic and diversified carbonaceous compression fossils from the Tonian Shiwangzhuang Formation in western Shandong, North China. Precambr. Res. 346, 105801 https://doi.org/10.1016/j.precamres.2020.105801.

Li, M., Vandyk, T.M., Wu, G., Liu, W., Le Heron, D.P., Xiao, Y., 2020b. A window into the Great Unconformity: Insights from geochemistry and geochronology of Ediacaran glaciogenic rocks in the North China Craton. J. Asian Earth Sci. 194, 104327 https://doi.org/10.1016/j.jseaes.2020.104327.

Li, X.-Y., Li, S., Wang, T.-S., Dong, Y., Liu, X.-G., Zhao, S.-J., Wang, K., Sun, J.-P., Dai, L.-M., Suo, Y.-H., 2020c. Geochemistry and detrital zircon records of the Ruyang-Luoyu groups, southern North China Craton: provenance, crustal evolution and Paleo-Mesoproterozoic tectonic implications. Geosci. Front. 11, 679–696. https://doi.org/10.1016/j.gsf.2019.08.003.

Liu, J., Liu, F., Ding, Z., Yang, H., Liu, C., Liu, P., Xiao, L., Zhao, L., Geng, J., 2013. U-Pb dating and Hf isotope study of detrital zircons from the Zhifu Group, Jiaobei Terrane, North China Craton: provenance and implications for Precambrian crustal growth and recycling. Precambr. Res. 235, 230–250. https://doi.org/10.1016/j.precamres.2013.06.014.

Mángano, M.G., Buatois, L.A., 2017. The Cambrian revolutions: trace-fossil record, timing, links and geobiological impact. Earth Sci. Rev. 173, 96–108. https://doi.org/10.1016/j.earscirev.2017.08.009.

McKenzie, N.R., Hughes, N.C., Myrow, P.M., Choi, D.K., Park, T.-Y., 2011. Trilobites and zircons link north China with the eastern Himalaya during the Cambrian. Geology 39, 591–594. https://doi.org/10.1130/g31838.1.

Meert, J.G., Lieberman, B.S., 2008. The Neoproterozoic assembly of Gondwana and its relationship to the Ediacaran-Cambrian radiation. Gondwana Res. 14, 5–21. https://doi.org/10.1016/j.gr.2007.06.007.

Meng, Q.-R., Wei, H.-H., Qu, Y.-Q., Ma, S.-X., 2011. Stratigraphic and sedimentary records of the rift to drift evolution of the northern North China craton at the Paleo- to Mesoproterozoic transition. Gondwana Res. 20, 205–218. https://doi.org/10.1016/j.gr.2010.12.010.

Meng, X., Ge, M., Tucker, M.E., 1997. Sequence stratigraphy, sea-level changes and depositional systems in the Cambro-Ordovician of the North China carbonate platform. Sed. Geol. 114, 189–222. https://doi.org/10.1016/s0037-0738(97)00073-0.

Oh, M.-K., 2020. Sedimentology of the Hydrothermally Altered Myobong Formation (lower Cambrian), Taebaek, Korea. M.S. Thesis. Chungnam National University, p. 67.

Parnell, J., Mark, D.F., Frei, R., Fallick, A.E., Ellam, R.M., 2014. $^{40}Ar/^{39}Ar$ dating of exceptional concentration of metals by weathering of Precambrian rocks at the Precambrian-Cambrian boundary. Precambr. Res. 246, 54–63. https://doi.org/10.1016/j.precamres.2014.02.012.

Paton, C., Hellstrom, J., Paul, B., Woodhead, J., Hergt, J., 2011. Iolite: Freeware for the visualisation and processing of mass spectrometric data. J. Anal. At. Spectrom. 26, 2508. https://doi.org/10.1039/c1ja10172b.

Paton, C., Woodhead, J.D., Hellstrom, J.C., Hergt, J.M., Greig, A., Maas, R., 2010. Improved laser ablation U-Pb zircon geochronology through robust downhole fractionation correction. Geochem. Geophys. Geosyst. 11, Q0AA06. https://doi.org/10.1029/2009gc002618.

Peng, S., Babcock, L.E., Cooper, R.A., 2012. The Cambrian Period. In: F.M. Gradstein , J. G. Ogg, M. Schmitz, G. Ogg (Eds.), The Geologic Time Scale 2012, Elsevier, pp. 437-488. 10.1016/b978-0-444-59425-9.00019-6.

Peters, S.E., Gaines, R.R., 2012. Formation of the 'Great Unconformity' as a trigger for the Cambrian explosion. Nature 484, 363–366. https://doi.org/10.1038/nature10969.

Peterson, D.O., Clark, D.L., 1974. Trace fossils *Plagiogmus* and *Skolithos* in the Tintic Quartzite (middle Cambrian) of Utah. J. Paleontol. 48, 766–768. https://doi.org/10.2307/1303227.

Petrus, J.A., Kamber, B.S., 2012. VizualAge: a novel approach to laser ablation ICP-MS U-Pb geochronology data reduction. Geostand. Geoanal. Res. 36, 247–270. https://doi.org/10.1111/j.1751-908X.2012.00158.x.

Pruss, S.B., Finnegan, S., Fischer, W.W., Knoll, A.H., 2010. Carbonates in skeleton-poor seas: New insights from Cambrian and Ordovician strata of Laurentia. Palaios 25, 73–84. https://doi.org/10.2110/palo.2009.p09-101r.

Seilacher, A., 1999. Biomat-related lifestyles in the Precambrian. Palaios 14, 86–93. https://doi.org/10.2307/3515363.

Shahkarami, S., Buatois, L.A., Mángano, M.G., Hagadorn, J.W., Almond, J., 2020. The Ediacaran-Cambrian boundary: evaluating stratigraphic completeness and the Great Unconformity. Precambr. Res. 345, 105721 https://doi.org/10.1016/j.precamres.2020.105721.

Son, C.M., Cheong, C.H., 1965. Sedimentary environment and geologic structure of Taebaegsan region. Seoul Univ. J. 15, 1–31 (in Korean with English abstract).

Steiger, R.H., Jäger, E., 1977. Subcommission on geochronology: convention on the use of decay constants in geo- and cosmochronology. Earth Planet. Sci. Lett. 36, 359–362. https://doi.org/10.1016/0012-821X(77)90060-7.

Tarhan, L.G., Droser, M.L., Planavsky, N.J., Johnston, D.T., 2015. Protracted development of bioturbation through the early Palaeozoic Era. Nat. Geosci. 8, 865–869. https://doi.org/10.1038/ngeo2537.

Tucker, M.E., 1992. The Precambrian-Cambrian boundary: seawater chemistry, ocean circulation and nutrient supply in metazoan evolution, extinction and biomineralization. J. Geol. Soc. 149, 655–668. https://doi.org/10.1144/gsjgs.149.4.0655.

Uhmb, T.-H., 2018. Deformation-Induced Right-Side-up Pseudostratigraphy in the early Paleozoic Joseon Supergroup of Southeastern Danyang area, South Korea. M.S. Thesis. Korea University, p. 88.

Vermeesch, P., 2013. Multi-sample comparison of detrital age distributions. Chem. Geol. 341, 140–146. https://doi.org/10.1016/j.chemgeo.2013.01.010.

Vermeesch, P., Resentini, A., Garzanti, E., 2016. An R package for statistical provenance analysis. Sed. Geol. 336, 14–25. https://doi.org/10.1016/j.sedgeo.2016.01.009.

Wan, B., Tang, Q., Pang, K., Wang, X., Bao, Z., Meng, F., Zhou, C., Yuan, X., Hua, H., Xiao, S., 2019. Repositioning the Great Unconformity at the southeastern margin of the North China Craton. Precambr. Res. 324, 1–17. https://doi.org/10.1016/j.precamres.2019.01.014.

Wan, Y., Liu, D., Wang, W., Song, T., Kröner, A., Dong, C., Zhou, H., Yin, X., 2011. Provenance of Meso- to Neoproterozoic cover sediments at the Ming Tombs, Beijing, North China Craton: An integrated study of U-Pb dating and Hf isotopic measurement of detrital zircons and whole-rock geochemistry. Gondwana Res. 20, 219–242. https://doi.org/10.1016/j.gr.2011.02.009.

Wiedenbeck, M., Allé, P., Corfu, F., Griffin, W.L., Meier, M., Oberli, F., Von Quadt, A., Roddick, J.C., Spiegel, W., 1995. Three natural zircon standards for U-Th-Pb, Lu-Hf, trace element and REE analyses. Geostand. Newsl. 19, 1–23. https://doi.org/10.1111/j.1751-908X.1995.tb00147.x.

Woo, J., Shinn, Y.J., Kwon, Y.K., Chough, S.K., 2006. The Jangsan and Myeonsan Formations (Early Cambrian) of the Taebaek Group, mideast Korea: depositional processes and environments. Geosci. J. 10, 35–57. https://doi.org/10.1007/BF02910331.

Xiao, S., Knoll, A.H., Kaufman, A.J., Yin, L., Zhang, Y., 1997. Neoproterozoic fossils in Mesoproterozoic rocks? chemostratigraphic resolution of a biostratigraphic conundrum from the North China Platform. Precambr. Res. 84, 197–220. https://doi.org/10.1016/S0301-9268(97)00029-6.

Xiao, S., Shen, B., Tang, Q., Kaufman, A.J., Yuan, X., Li, J., Qian, M., 2014. Biostratigraphic and chemostratigraphic constraints on the age of early Neoproterozoic carbonate successions in North China. Precambr. Res. 246, 208–225. https://doi.org/10.1016/j.precamres.2014.03.004.

Yin, A., Nie, S., 1993. An indentation model for the North and South China collision and the development of the Tan-Lu and Honam Fault Systems, eastern Asia. Tectonics 12, 801–813. https://doi.org/10.1029/93TC00313.

Yun, S., 1978. Petrography, chemical composition, and depositional environments of the Cambro-Ordovician sedimentary sequence in the Yeonhwa I Mine area, southeastern Taebaegsan Region, Korea. J. Geol. Soc. Korea 14, 145–174.

Zhai, M., Zhang, X.-H., Zhang, Y.-B., Wu, F.-Y., Peng, P., Li, Q.-L., Li, Z., Guo, J., Li, T.-S., Zhao, L., Zhou, L.-G., Zhu, X., 2019. The geology of North Korea: an overview. Earth Sci. Rev. 194, 57–96. https://doi.org/10.1016/j.earscirev.2019.04.025.

Zhang, T., Myrow, P.M., Fike, D.A., McKenzie, N.R., Yuan, J., Zhu, X., Li, W., Chen, J., 2020. Sedimentology, stratigraphy, and detrital zircon geochronology of Mesoproterozoic strata in the northern Helan Mountains, western margin of the North China Block. Precambr. Res. 343, 105730 https://doi.org/10.1016/j.precamres.2020.105730.

Zhang, X., Ahlberg, P., Babcock, L.E., Choi, D.K., Geyer, G., Gozalo, R., Stewart Hollingsworth, J., Li, G., Naimark, E.B., Pegel, T., Steiner, M., Wotte, T., Zhang, Z., 2017. Challenges in defining the base of Cambrian Series 2 and Stage 3. Earth Sci. Rev. 172, 124–139. https://doi.org/10.1016/j.earscirev.2017.07.017.

Zhao, G., Sun, M., Wilde, S.A., Sanzhong, L., 2005. Late Archean to Paleoproterozoic evolution of the North China Craton: key issues revisited. Precambr. Res. 136, 177–202. https://doi.org/10.1016/j.precamres.2004.10.002.

Zhao, H., Zhang, S., Zhu, M., Ding, J., Li, H., Yang, T., Wu, H., 2021. Paleomagnetic insights into the Cambrian biogeographic conundrum: did the North China craton link Laurentia and East Gondwana? Geology 49, 372–376. https://doi.org/10.1130/g47932.1.

Zhen, Y.Y., Zhang, Y., Wang, Z., Percival, I.G., 2016. Huaiyuan Epeirogeny—Shaping Ordovician stratigraphy and sedimentation on the North China Platform. Palaeogeogr. Palaeoclimatol. Palaeoecol. 448, 363–370. https://doi.org/10.1016/j.palaeo.2015.07.040.

Zuo, P., Li, Y., Zhang, G., Si, R., Wang, S., Liu, S., Zheng, D., Sun, J., 2019. Reviews of the Mesoproterozoic to Neoproterozoic sedimentary sequences and new constraints on the tectono-sedimentary evolution of the southern margin of the North China Craton. J. Asian Earth Sci. 179, 416–429. https://doi.org/10.1016/j.jseaes.2019.04.010.